LHAASO天体辐射与宇宙线成分谱观测研究及新探测技术研究

课题二：“膝区”宇宙线物理研究

报告人：张兵（高能所）

课题承担单位：中国科学院高能物理研究所

课题参与单位：北京大学

国家重点研发计划2026年度会议，山东青岛，2026/08/17

The spectrum of cosmic rays

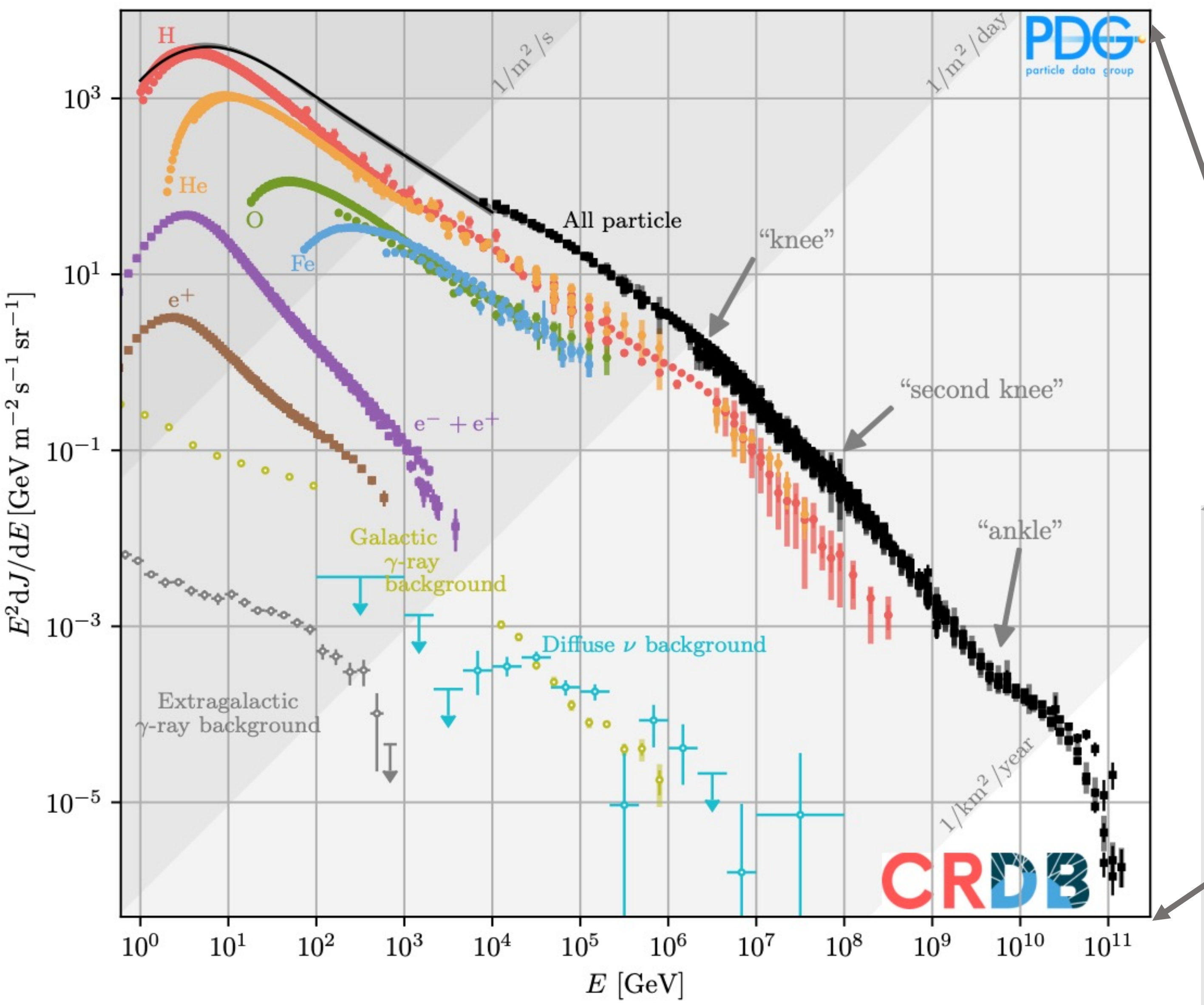

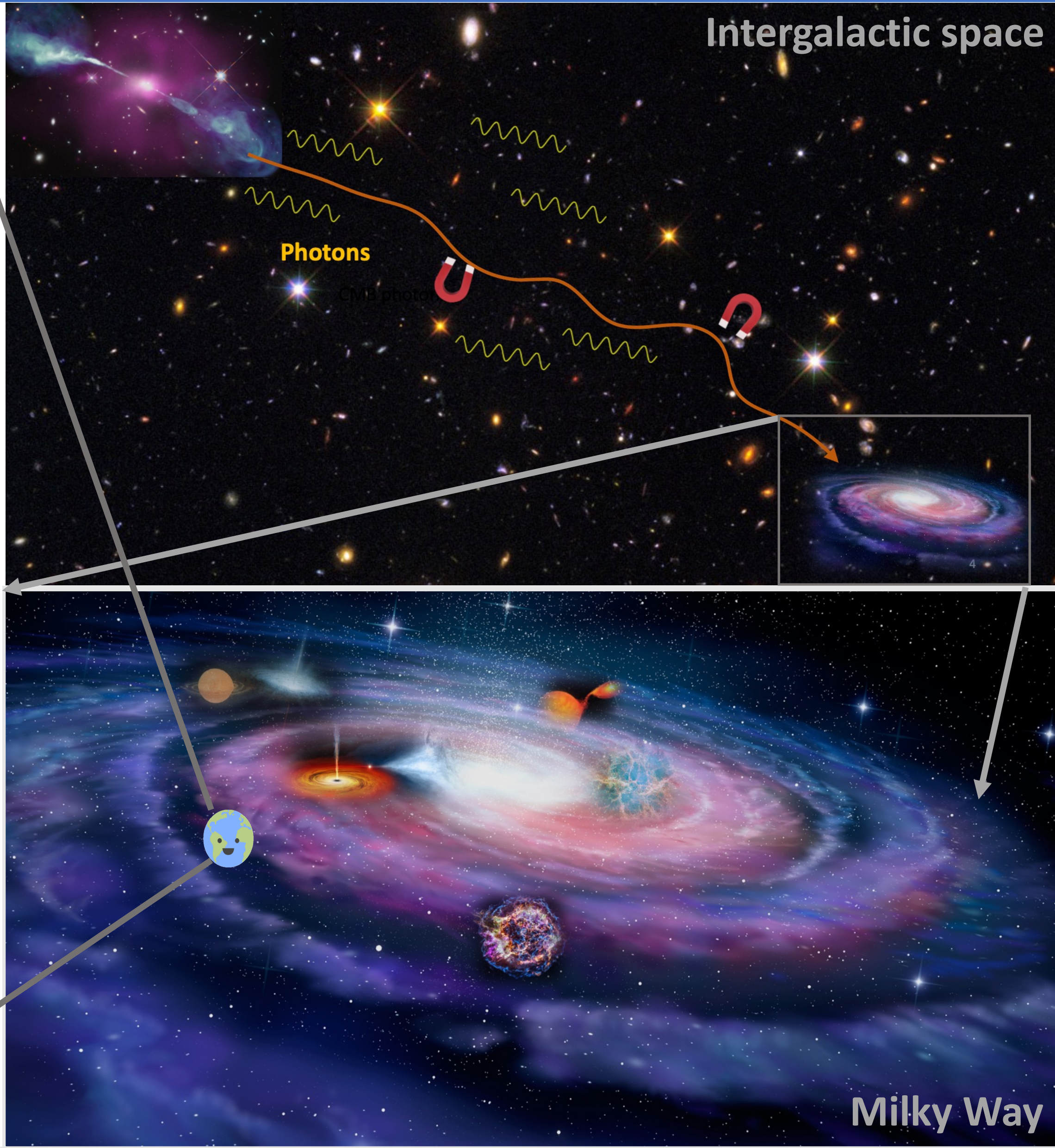

Cosmic Ray Anisotropy

Local B field

Galactic Center

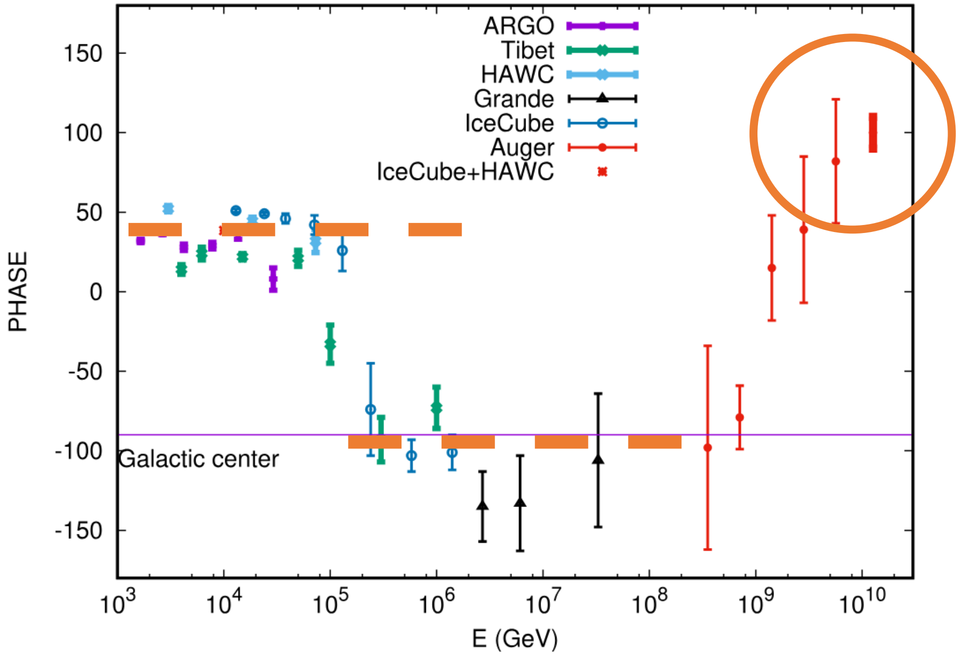

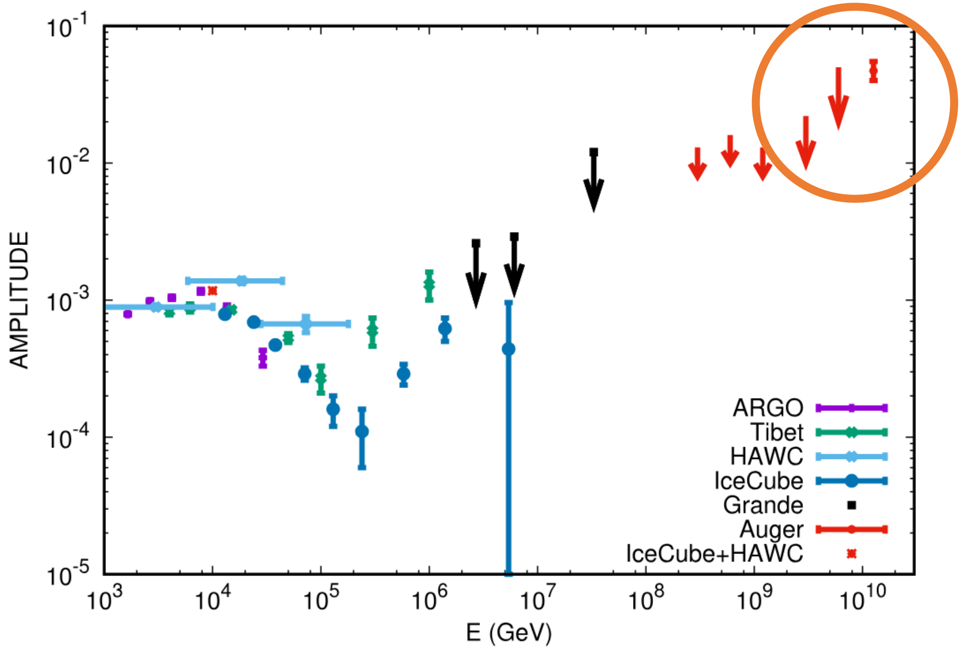

Auger Dipole

[e.g., Kachelriess & Semikoz, 2019]

- The detection of a dipolar anisotropy at energies above 8 EeV marks the evidence that the majority of sources of UHECRs are not in the Milky Way (~120 degree away from the Galactic center ）极高能宇宙线来自银河系外的天体

第二课题：研究内容

一："膝区"结构成因

- 宇宙线在银河系内的传播
- 能谱、成分和各向异性随能量的演化

二："膝区"宇宙线的加速源在哪里？

- PeV宇宙线加速源的多波段多信使研究
- 宇宙线成分、加速机制与近源区传播的研究

三：宇宙线从河内到河外的过渡

- 河外宇宙线加速源的多波段多信使研究
- 宇宙线从河内到河外的过渡过程

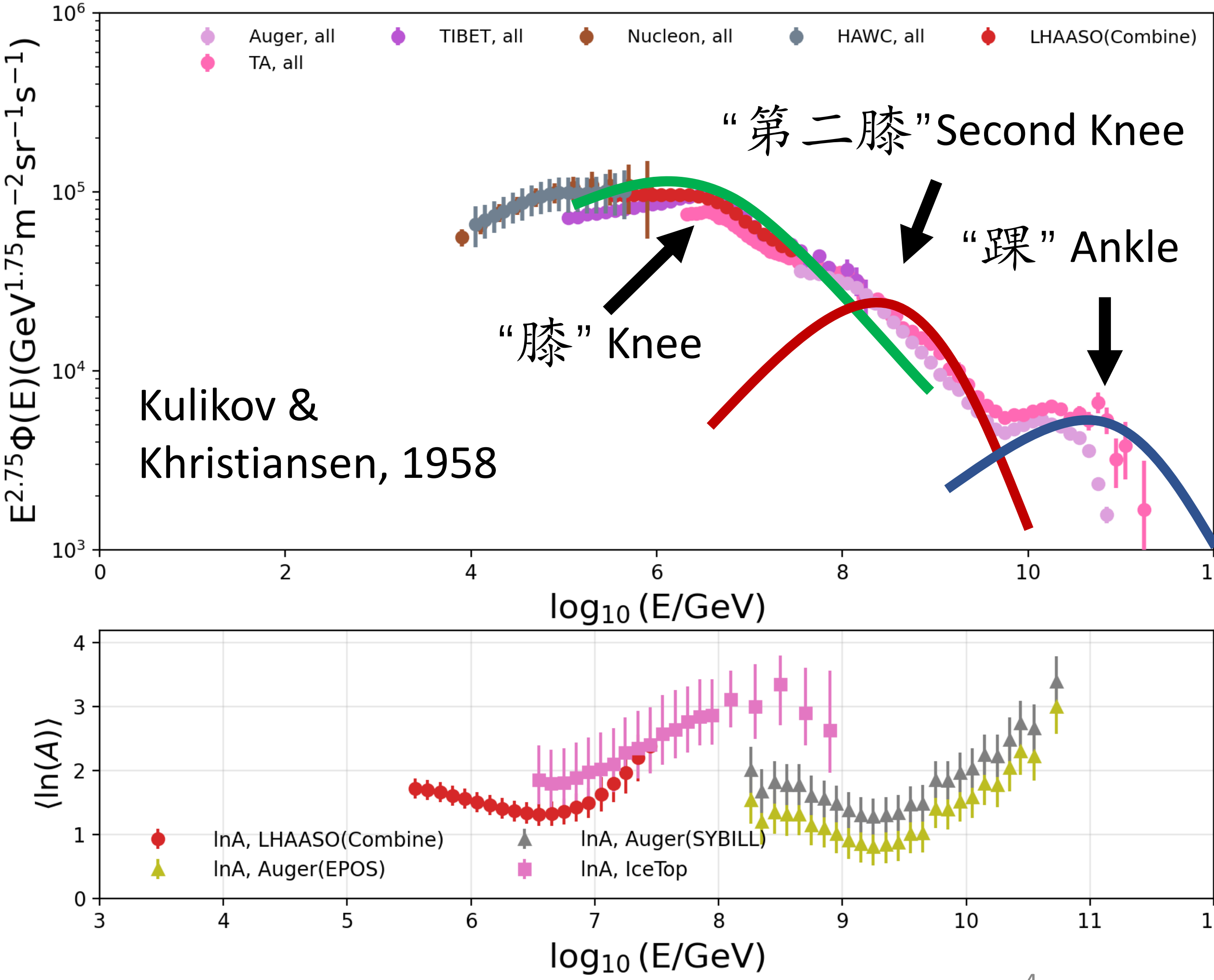

Cosmic ray proton and helium spectrum

Insights from Cosmic ray proton and helium observation

Progress on cosmic ray proton spectrum

Galactic CR proton spectrum is not single powerlaw, but show complex hardening and steeping features

- The all-particle ``knee'' is related to the steeping of the proton spectrum
- The steeping in the proton spectrum reflects the upper energy limits of Galactic particle accelerators (few PeV)

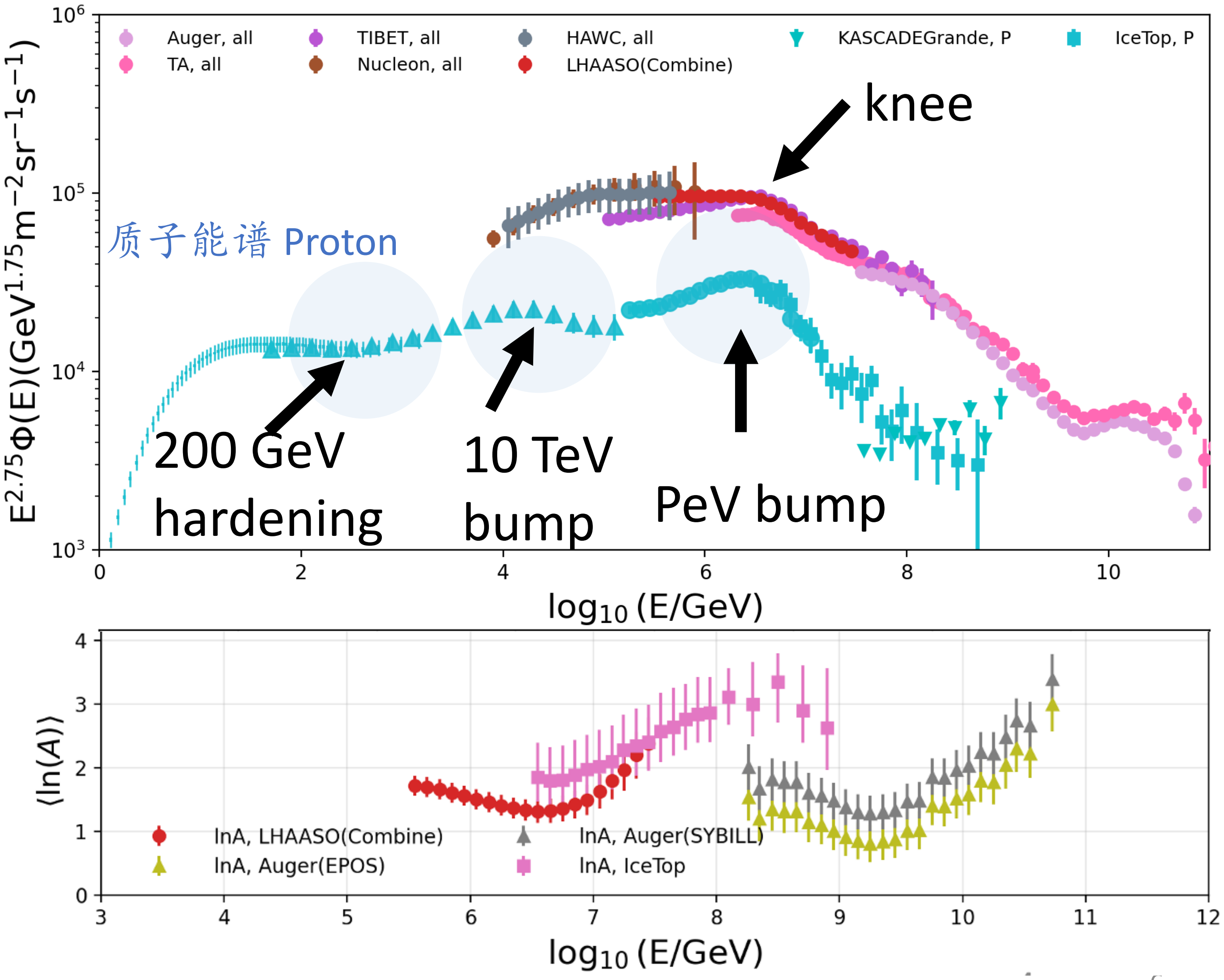

Progress on cosmic ray helium spectrum

Changes of proton/helium composition ratio implicates different source environment

At the ``knee'', proton dominate over helium

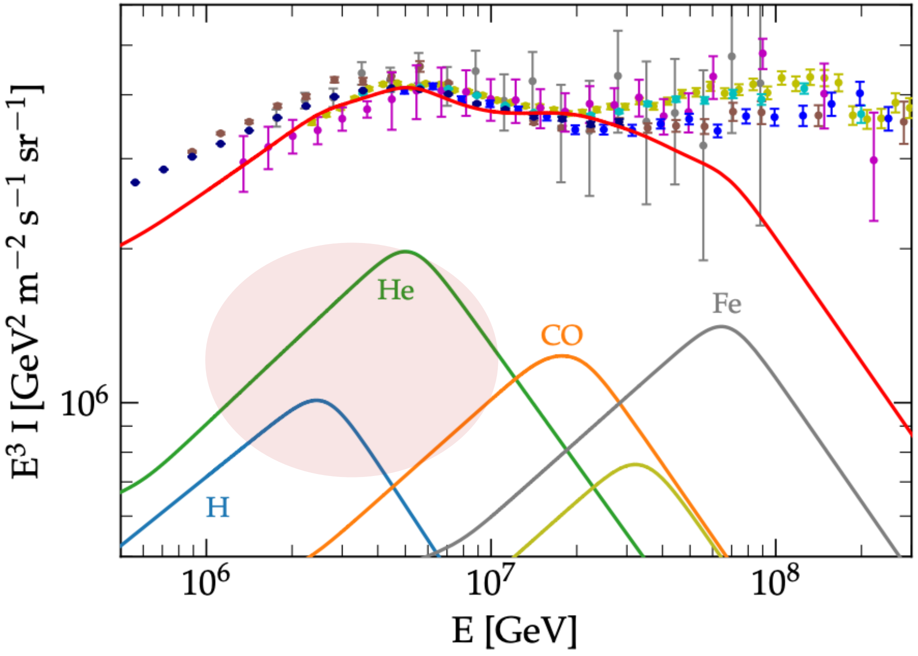

By Carmelo Evoli, 2024 (Fitting based on helium component dominated ``knee'')

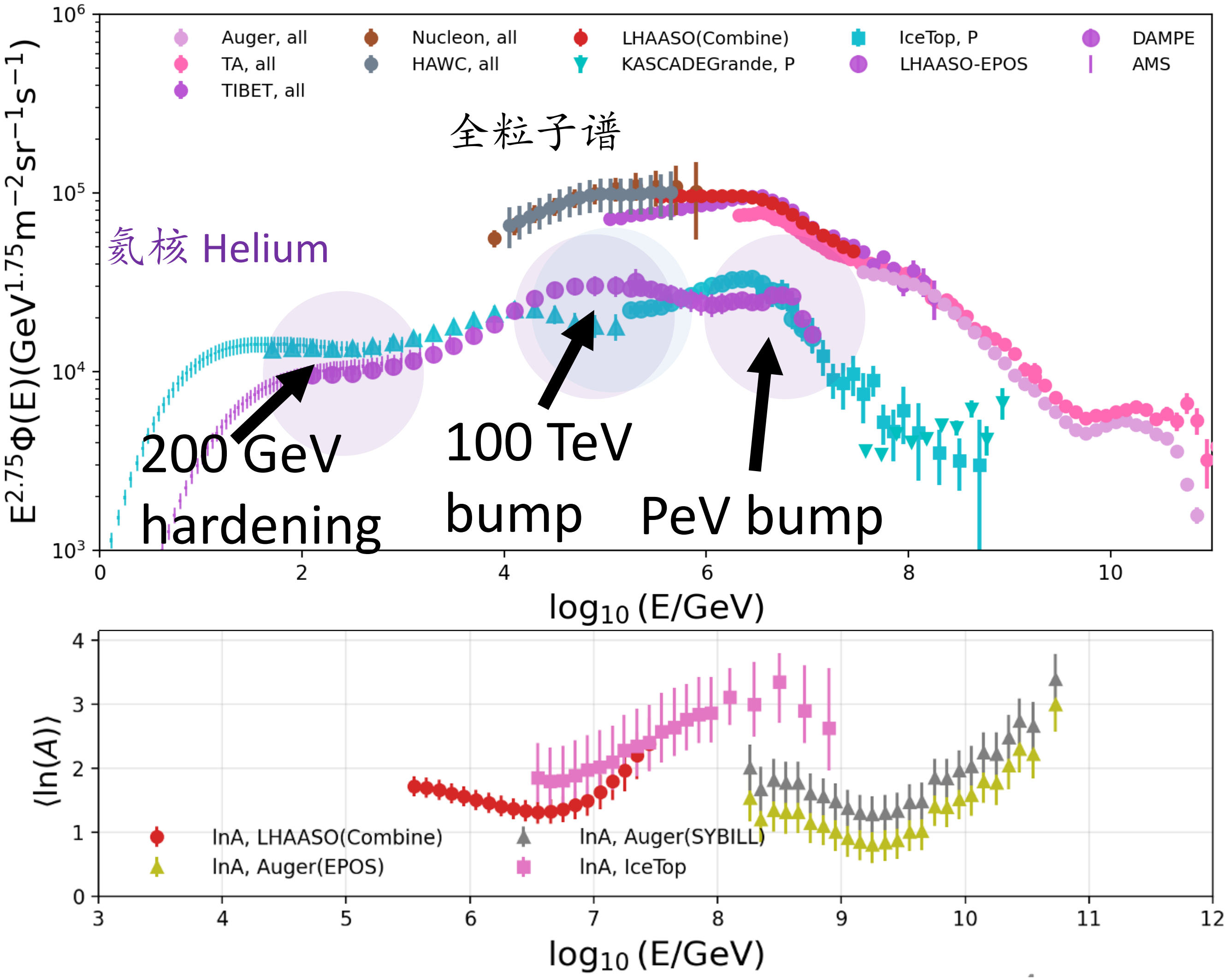

Research progress

1、银河系宇宙线的起源与传播

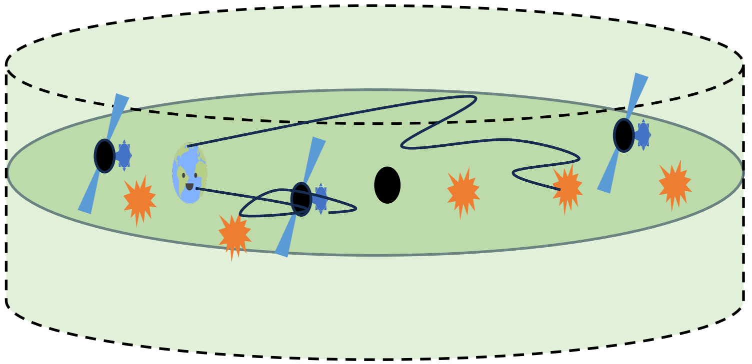

- B. T. Zhang & Yu, Microquasar remnants as Pevatrons Illuminating the Galactic Cosmic Ray Knee, PRL under review, 2026
  - 微类星体遗迹解释PeV宇宙线质子能谱
- Aharonian & B. T. Zhang, A Minimal Interpretation of the Galactic Cosmic-Ray Proton and Helium Spectra from GeV to PeV Energies, ApJ, 2026
  - 从GeV到PeV的银河系宇宙线的双成分模型
- B. T. Zhang, Kimura & Murase, Microquasar jet-cocoon systems as PeVatrons, PRD, 2025
  - 微类星体剪切加速机制遗迹对宇宙线全粒子能谱、分成分能谱和成分的解释
- Yue, J. Zhang, …, Guo & Hu, X-Ray Binaries: A Potential Dominant Contributor to the Cosmic-Ray Spectral Knee Structure, ApJ, 2026
  - X射线双星与超新星遗迹解释宇宙线质子能谱
- Nie, Yue, Guo & Liu, A Multi-messenger Search for a Nearby Microquasar Contributor to the Cosmic Ray Knee, submitted, 2026
  - 来自已知的微类星体对于地球上观测的宇宙线流量的贡献
- Yue, Nie, Guo & Hu, Joint Constraint on the Propagation Origin of the Cosmic-Ray Spectral Knee from Energy Spectrum and Anisotropy Observations, ApJ, 2026
  - 限制银河系宇宙线“膝”区传播效应起源

Research progress

2、基于伽马射线和中微子研究银河系加速源的性质

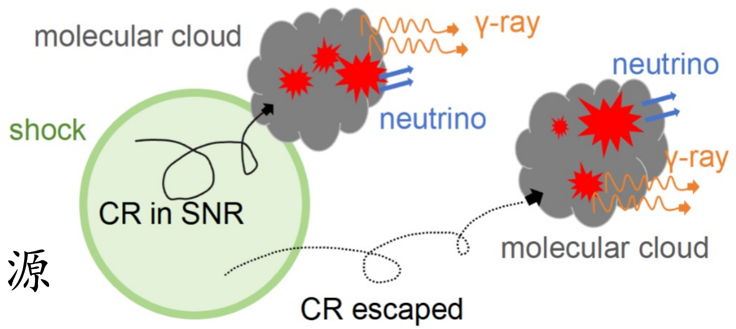

- LHAASO Collaboration, Extreme PeV accelerator associated with GRS 1915+105, ApJL under review, 2026
  - GRS 1915+105不仅是PeV加速源而且其中的伽马射线是强子起源
- Chen, B. T. Zhang, Xin & Liu, Constraining Cosmic-Ray Acceleration and Escape in Middle-Aged Supernova Remnants with GeV–TeV Gamma-Ray Observations, to be submitted to PRD, 2026
  - 通过高能/甚高能伽马射线数据限制超新星中宇宙线的加速与逃逸过程
- Yu & B. T. Zhang, Galactic Microquasar and Supernova Remnants Imprinting on the Diffuse Neutrino Sky, submitted to ApJL, 2026
  - 微类星体和超新星遗迹作为宇宙线加速源及其伴随的银河系弥散中微子和伽马射线
- Li, Wang & Li, Particle acceleration in Cassiopeia A revealed by the broadband high-energy spectrum, PRD, 2026
  - Cas A中宇宙线的加速以及作为PeV宇宙线的潜在候选源
- Nie, Guo & Liu, A Possible Common Physics Picture Reflected by the Gamma-Ray Emission of the Galactic Center, ApJ, 2025
  - 银心伽马射线起源于低能背景宇宙线以及过去活跃期加速的高能宇宙线的共同作用
- Nie, Ge, Guo & Liu, Geminga: A Window into the Role Played by the Local Halo in the Cosmic-Ray Propagation Process, ApJ, 2025; Nie, Guo & Liu, two-component γ-Ray Structure from the CR Sources Within Dense Clouds, submitted to JCAP, 2026

Research progress

3、宇宙线从河内到河外的过渡以及河外宇宙线加速源

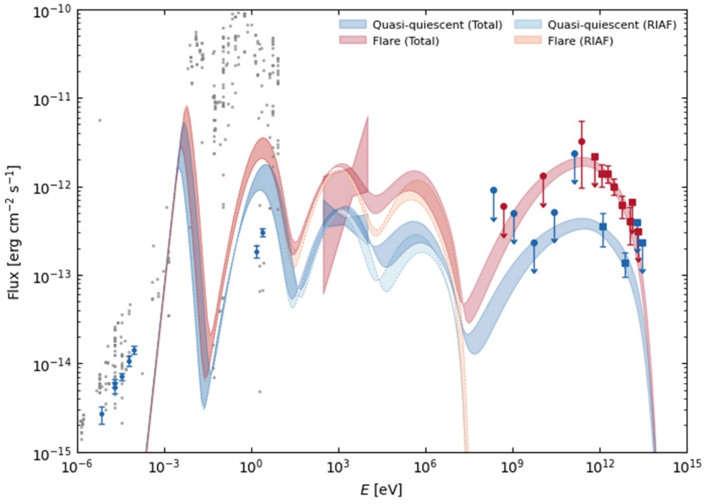

河外（低光度）伽马暴产生极高能中微子以及作为极高能宇宙线加速源

- Q. Zhang, Huang & Li, Overall Ultra-high Energy Neutrino Emission from GRBs During Jet Expansion, ApJ, 2025
- Yu & B. T. Zhang, Multimessenger Modeling of Low-luminosity gamma-Ray Bursts, ApJ, 2026
- Yu & B. T. Zhang, A Unified Framework for 10 TeV to EeV Diffuse Neutrino Sky and KM3-230213A, ApJL, 2026

低光度活动星系核NGC 4278中宇宙线加速以及甚高能伽马射线和中微子辐射机制研究

- Chen, Abhishek, B. T. Zhang, Physical Origin of Very-high-energy Gamma Rays from the Low-luminosity Active Galactic Nucleus NGC 4278 and Implications for Neutrino Observations, ApJ, 2026

Cosmic ray source

Source populations inferred from observed spectrum

Galactic source populations

[Aharonian and BTZ, 2026, ApJ]

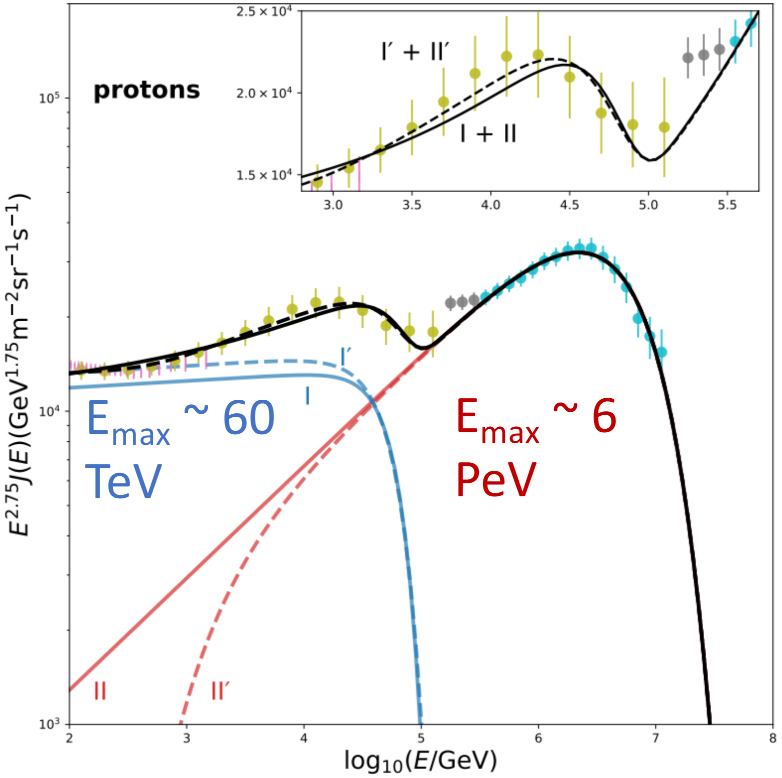

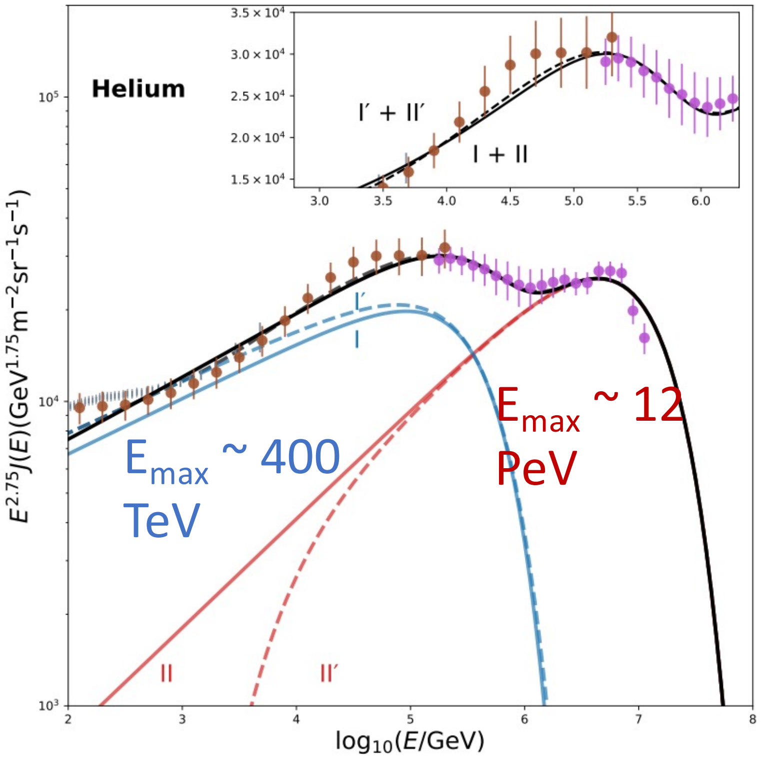

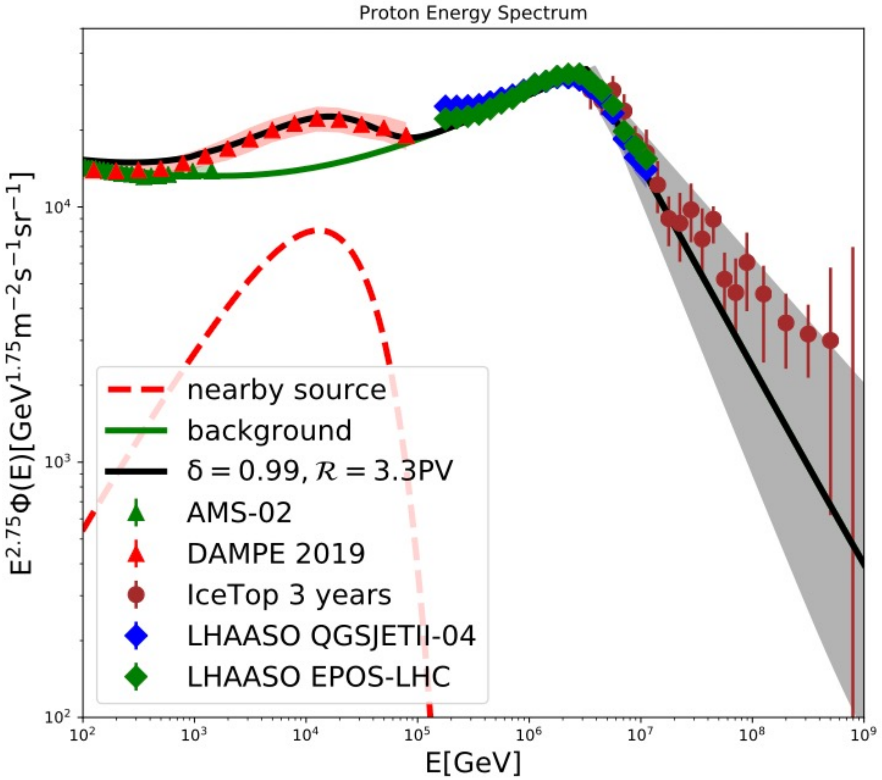

[Yue, Nie, Guo & Hu, 2026, ApJ]

[See also, DAMPE Coll. Nature, 2026; Yuan 2026]

The two-component model applied to CR proton and helium naturally explains the gradual spectral hardening

One and/or two source population with a nearby source?

Low-energy behavior below 100 GeV

[Aharonian and BTZ, 2026, ApJ]

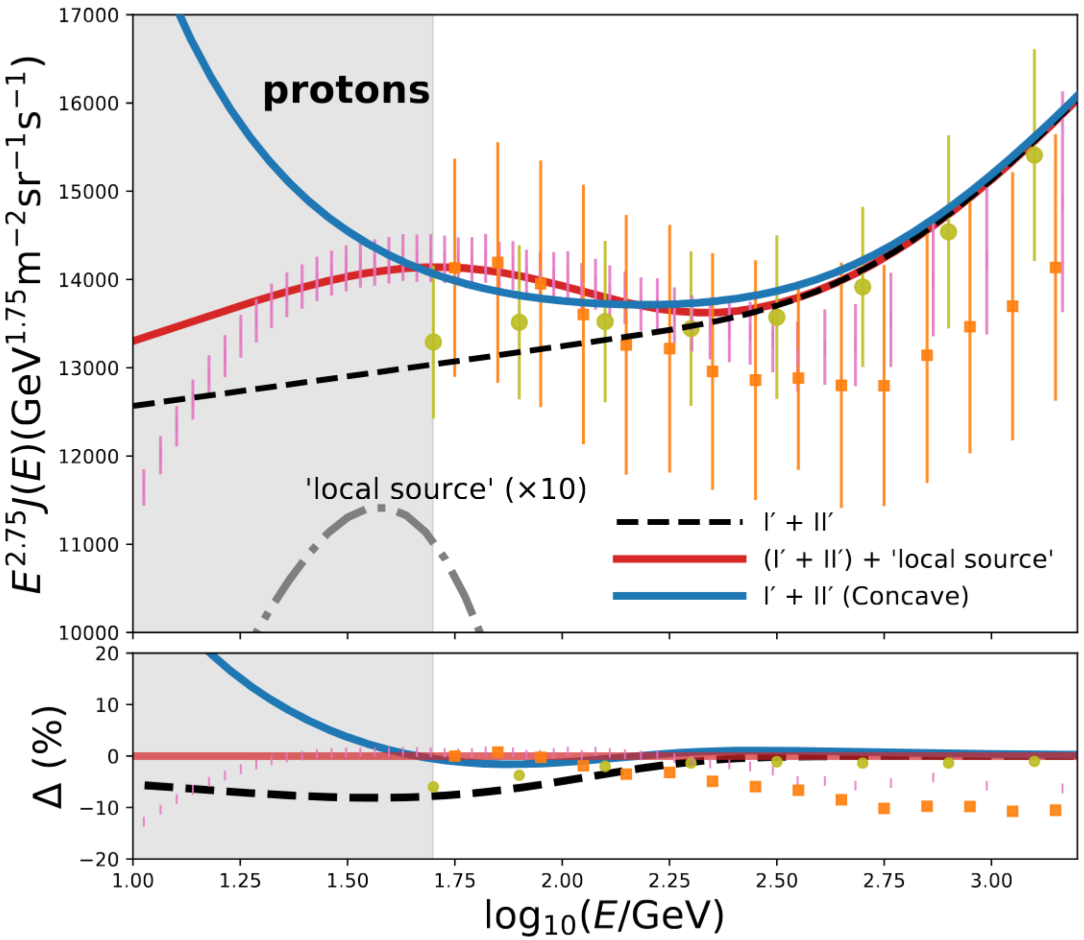

- A gradual low-energy steepening could arise from an additional nearby source contribution, reflect the contribution of local-source populations?

- Teflect the expected concavity of spectra produced within nonlinear DSA models
[V. Ptuskin et al. 2013; Zirakashvili et. al. 2014]

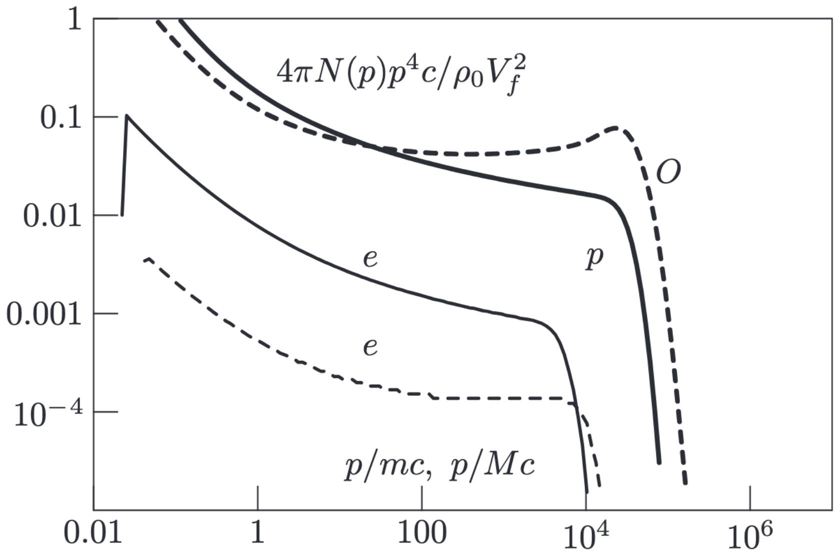

Cosmic ray sources

Physical properties of supernova remanants and microquasar

SNRs as Galactic cosmic ray sources

SNRs as the dominant source population responsible for Galactic CRs

- Observations of SNRs oftentimes show power law spectra non-thermal emission of X-rays [*Reynolds, 2008*]
- Diffusive shock acceleration work in SNR's blastwave

  [*Krymsky12; Bell13; Axford, Lear and Skadron14; Blandford and Ostriker; 1977-78*]
- The locally observed energy density of cosmic rays can be explained if on average ~ 10% of the shock kinetic energy is converted to GCRs

  [*Strong ApJL, 2010*]

However, SNR as sources of PeV energy CRs are challenged both from theory and observation !!!

Credit: Cassiopeia A by Chandra

Hoshino, PTPS, 2001

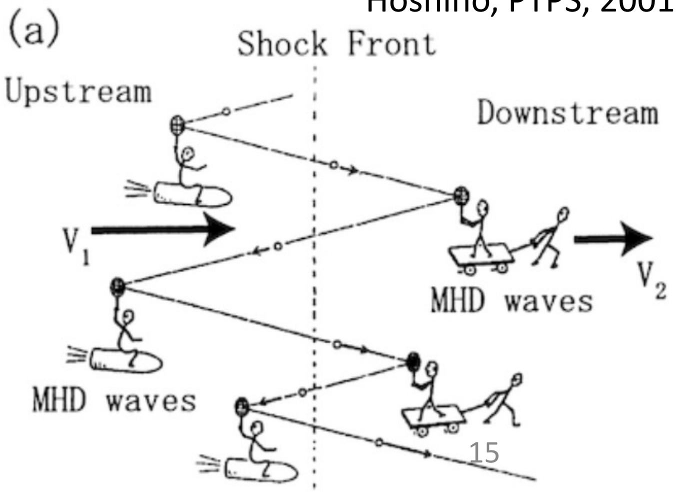

CR acceleration and escape from SNRs

[Chen, BTZ, Xing & Liu, 2026, to be submitted; see tomorrow's talk by Siyu Chen]

W 51 C

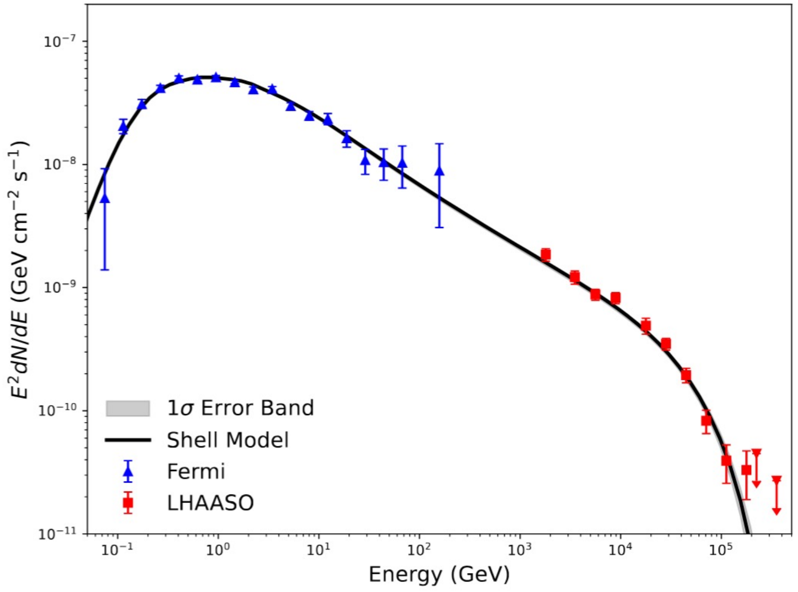

$$E_{\rm max} = 543^{+70}_{-59}\ {\rm TeV}, s_{\rm cr} = 2.00^{+0.005}_{-0.002}$$

W44

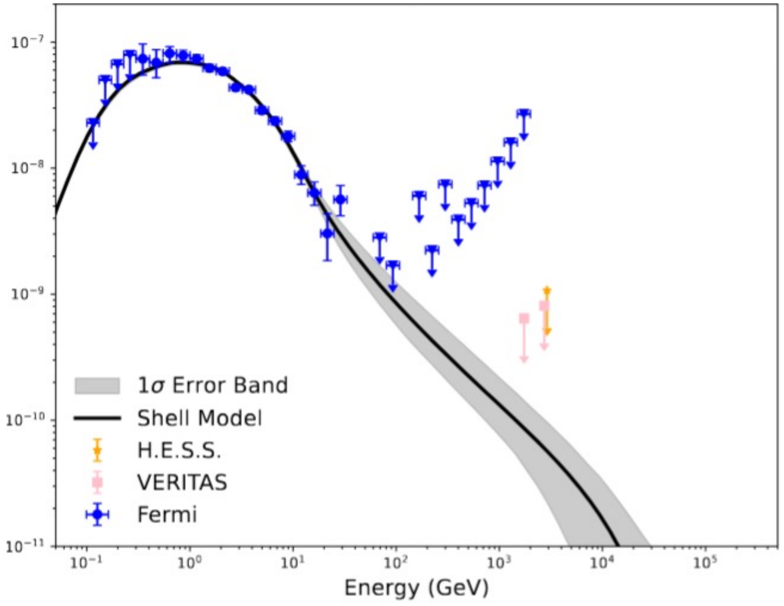

$$E_{\rm max} = 105^{+385}_{-83}\ {\rm TeV}, s_{\rm cr} = 2.25^{+0.06}_{-0.08}$$

IC 443

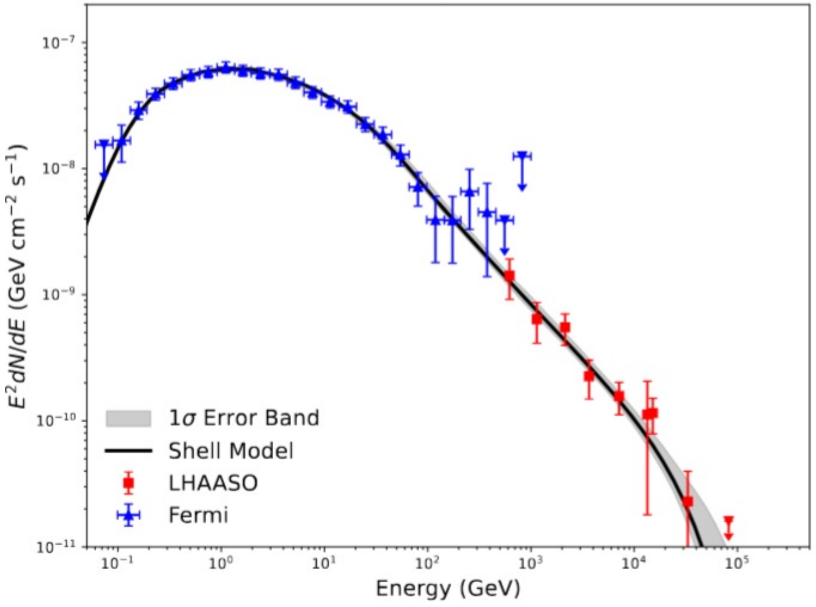

$$E_{\rm max} = 375^{+327}_{-183}\ {\rm TeV}, s_{\rm cr} = 2.34^{+0.03}_{-0.04}$$

A time-dependent modeling of the gamma-ray emission from four middle-aged SNRs, including both CRs confined within the remnant shells and escaped CRs interacting with ambient molecular clouds

Galactic PeVtron candidates

Galactic PeVtrons: 43 UHE gamma-ray sources (Cao et al. 2023)

Supernova remant (Some special or energetic SNRs?)

Pulsar wind neuble (Extreme accelerator, not evidence of hadronic interaction)

Microquasar (Powerful PeV accelerator, evidence of hadronic interaction)

Young Massive stellar cluster (Cygnus OB2?)

Galactic Center, Sgr A* (Powerful PeV accelerator?)

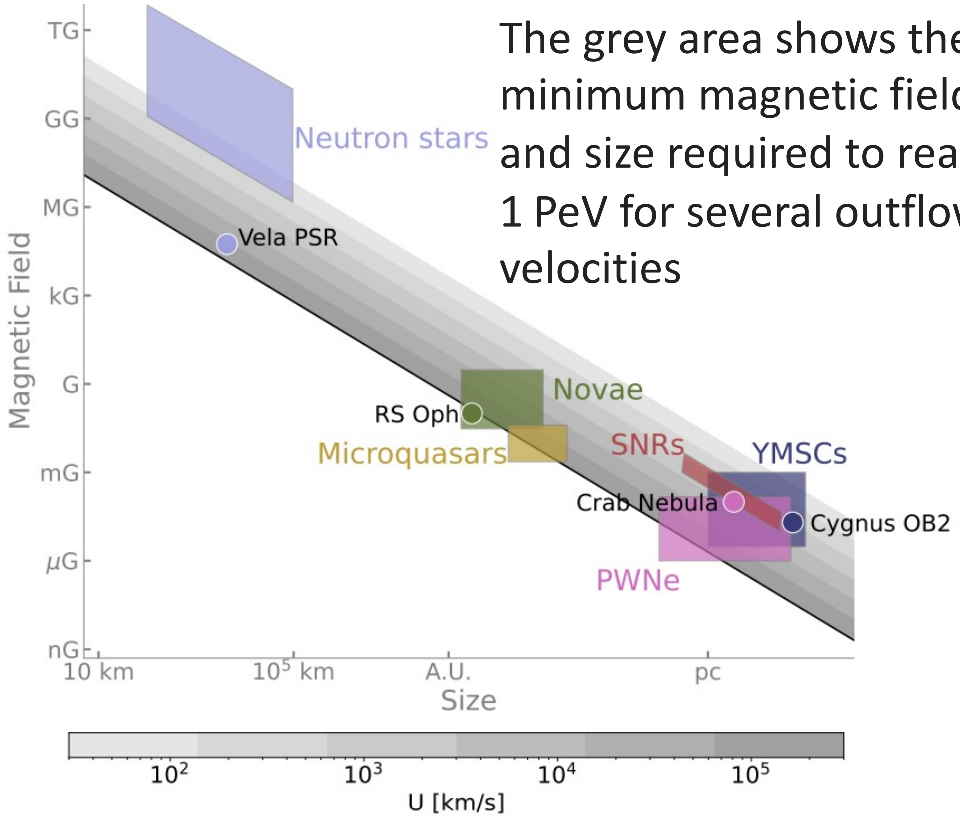

The grey area shows the minimum magnetic field and size required to reach 1 PeV for several outflow velocities

de Ona Wilhelmi et. al., 2024

$$E_{\max}^{\mathrm{th}} = Z\left(\frac{e}{c}\right) L\,U\,\mathcal{B}$$

$$\approx 0.3\,Z\left(\frac{L}{\mathrm{pc}}\right)\left(\frac{U}{1{,}000\,\mathrm{km\,s^{-1}}}\right)\left(\frac{\mathcal{B}}{100\,\mu\mathrm{G}}\right)\mathrm{PeV}$$

Microquasars

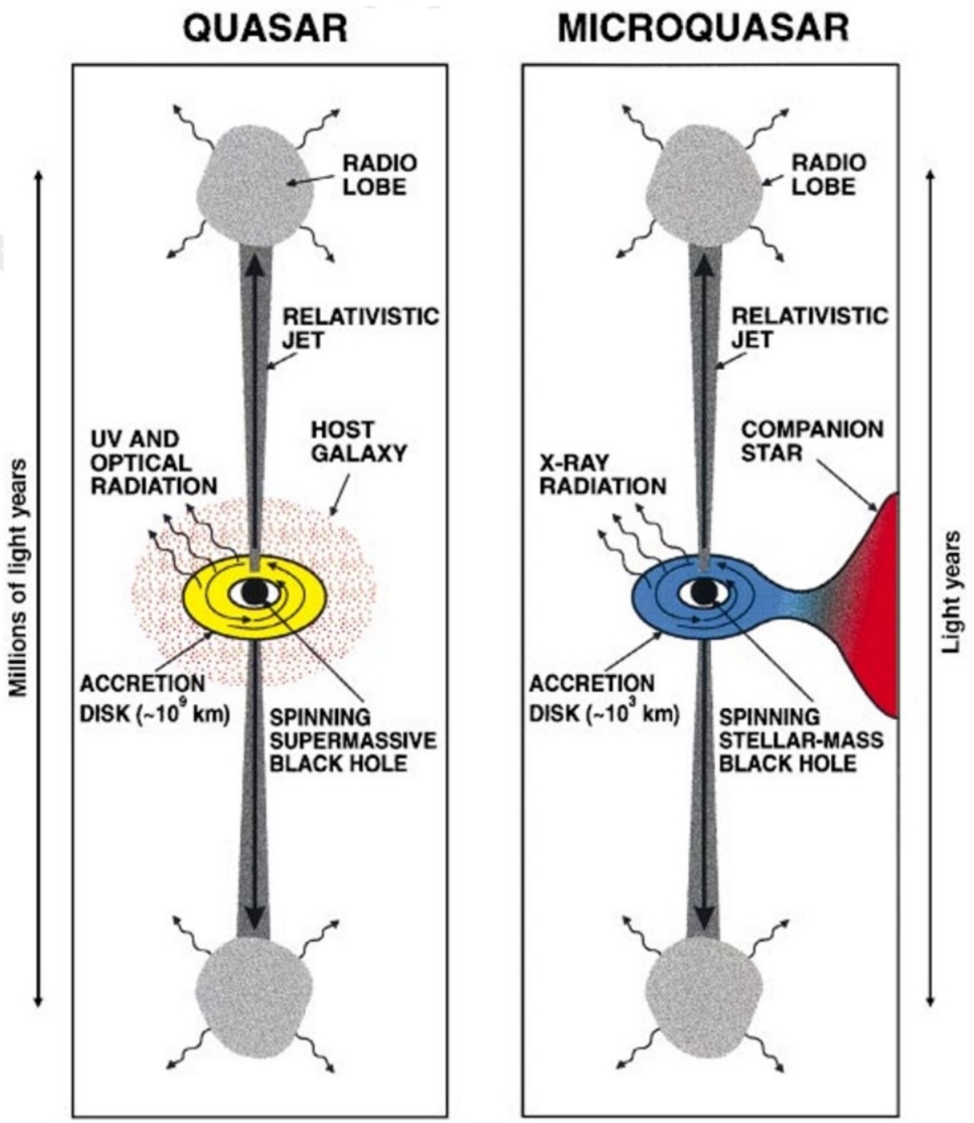

[*J. M. Paredes and J. Martí, 2003*]

- Microquasars are X-ray binaries with relativistic jets
- A microquasar consists of a compact object, usually a black hole, and a companion star
- Display phenomenology similar to active galactic nuclei (AGNs), although the size of the system is orders of magnitude different
- Around 20 microquasars found! At least, ~6 are detected in VHE-UHE band by HAWC, HESS and LHAASO

UHE gamma-ray energy spectrum from microquasars

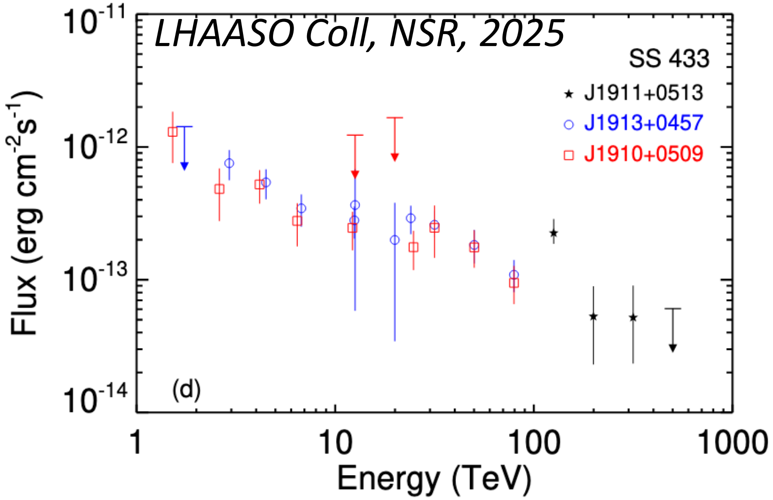

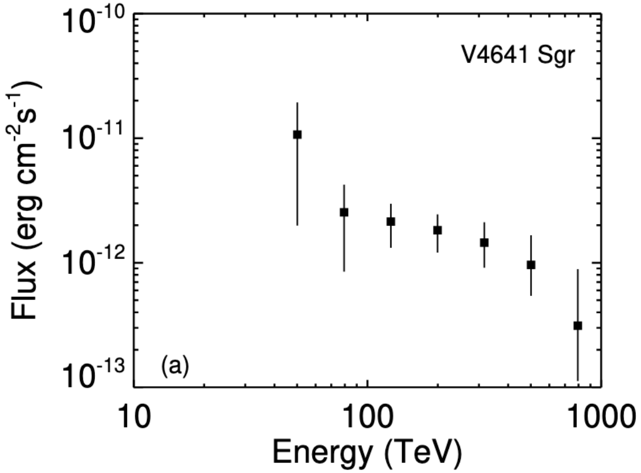

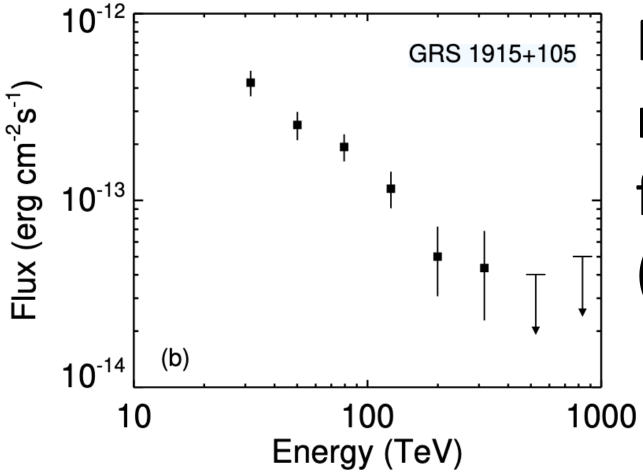

For gamma rays produced from hadronic (*pp)* process:

$$E_p \sim (3-10)E_\gamma$$

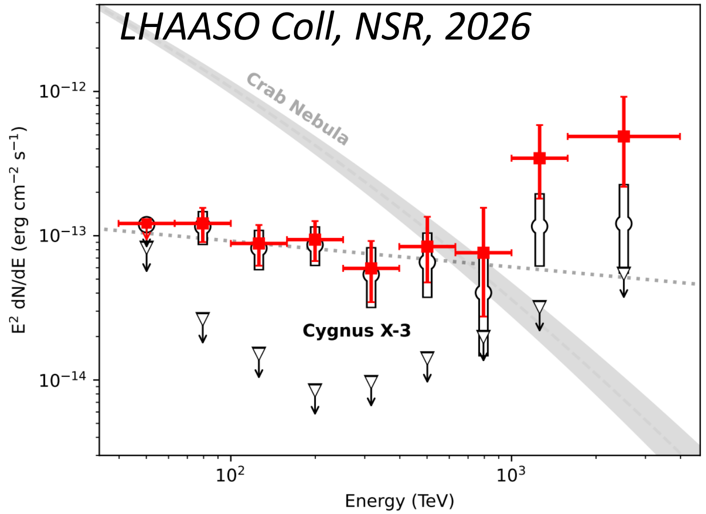

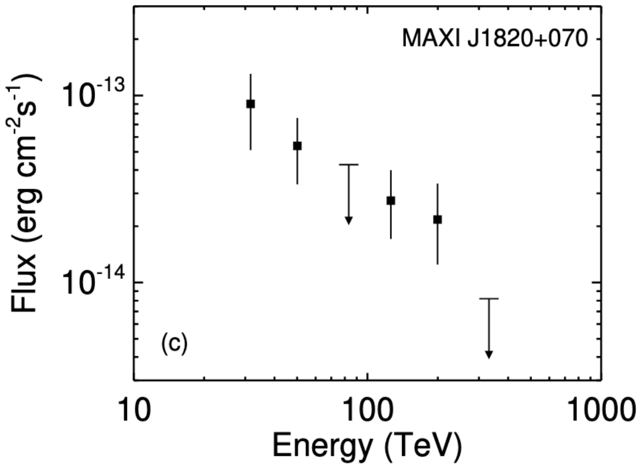

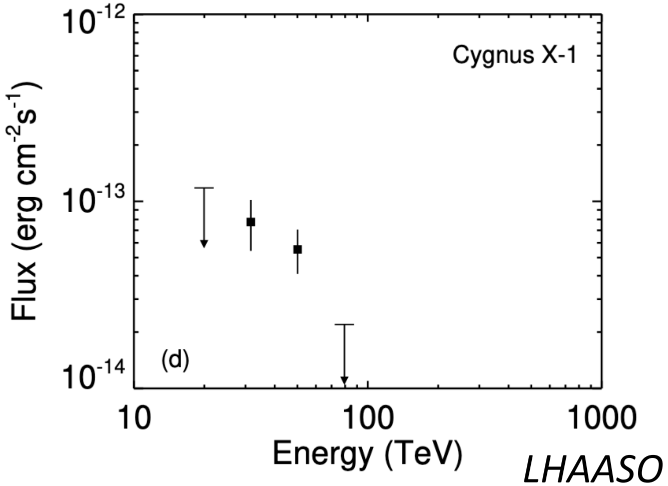

LHAASO Coll, NSR, 2024

Accreting BHs and their environments can operate as extremely efficient accelerators of particles out of 1 PeV

Hadronic origin of the broadband gamma-ray spectrum

Power law with exponential cutoff

$$\mathrm{d}N/\mathrm{d}E = AE^{-s_{\rm cr}}\exp(-E/E_{\rm max})$$

- Energy budget: $W_p \approx 7.9^{+2.7}_{-2.4} \times 10^{49}(n_{\rm gas}/100\,{\rm cm}^{-3})^{-1}$ erg
- Spectral index: $s_{\rm cr} = 2.4$
- Max proton energy: $E_{p,\rm max} \approx 5.1^{+12.7}_{-2.8}$ PeV

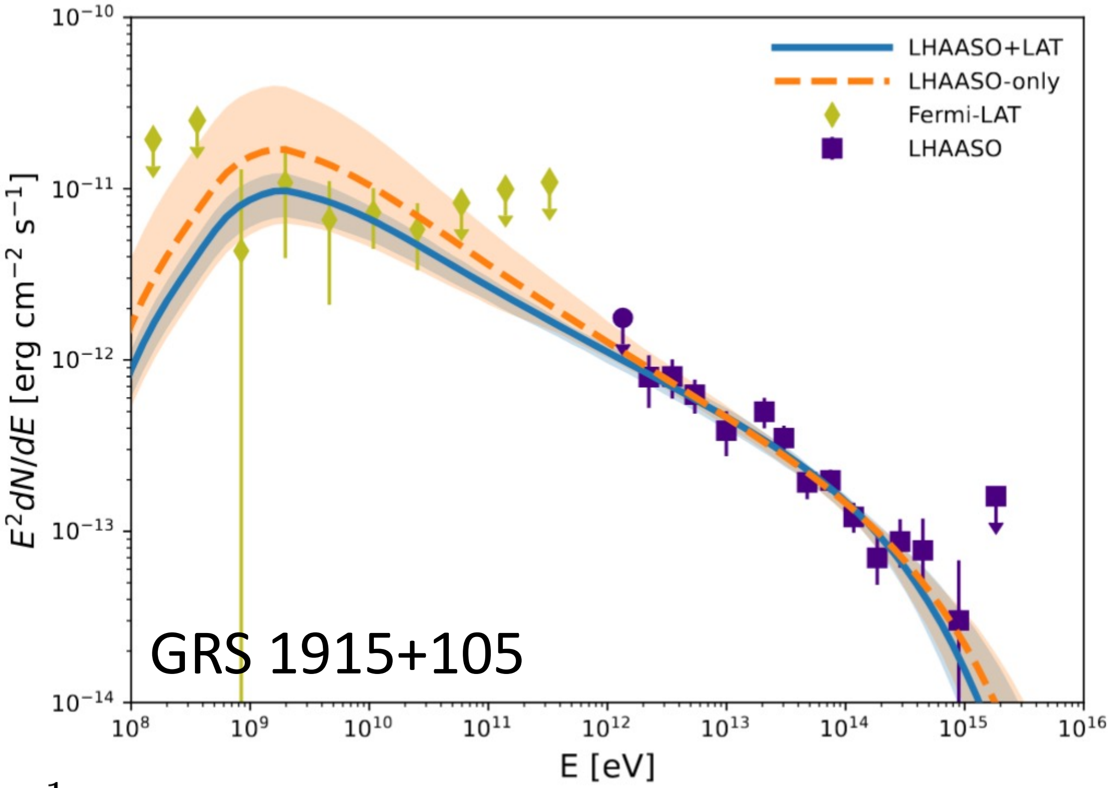

The required proton injection rate:

$$Q_p \approx W_p/t_{\rm age} \simeq 2.5\times 10^{37}\,(n_{\rm gas}/100\,{\rm cm}^{-3})^{-1}\,{\rm erg\ s}^{-1}$$

[LHAASO Collab., 2026, submitted]

Jet with an average kinetic luminosity: $\bar{L}_{\rm jet} \sim 10^{39}\,{\rm erg\ s}^{-1}$

Age: $t_{\rm age} = 0.1\,{\rm Myr}$

Conclusion: The dense environment favors hadronic process, and supported by LHAASO observations; The accelerated CRs have hard spectrum with $s_{\rm cr,acc} \sim 2$

Cosmic ray propagation

Modeling the propagation of CRs as diffusive process

Basic setup

[Zhang, Kimura & Murase, 2026, PRD]

We employ a publicly available version of the DRAGON code to propagate CRs

- The maximum value of Galactocentric radius is 10 kpc and halo size is 4 kpc

- The spatial distribution of the diffusion coefficient (Constrained from boron to carbon ratio)

$$D = 23.8 \times 10^{28} (\mathcal{R}/250\ \mathrm{GV})^{\delta} \mathrm{cm}^2\ \mathrm{s}^{-1} \quad \mathcal{R} \geqslant 250\ \mathrm{GV}, \delta = 1/3$$

The spatial distribution of microquasars is unknown, but high-Eddington ratio microquasars, including SS 433 or Sgr V4641, likely follow the distribution of massive stars

- Assume similar spatial distribution with Galactic SNRs (Ferriere2001) and adopt continuous source distribution

See also Galactic X-ray binary radial distribution
[Yue, J. Zhang, …, Guo & Hu, ApJ, 2026]

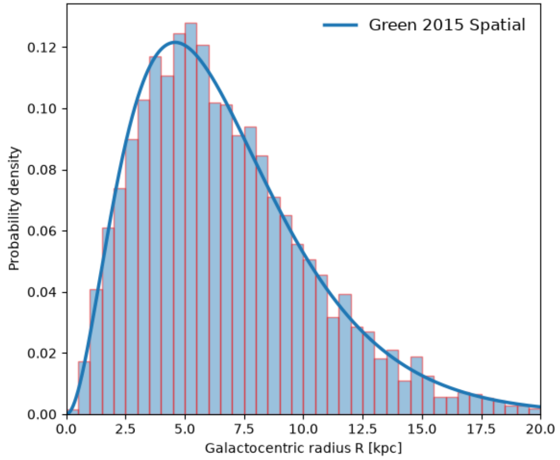

Cosmic ray acceleration

Shear acceleration

- A class of the Fermi acceleration, has been suggested to be an efficient mechanism to accelerate CRs
- Charged particles gain energy inside an ordered shear velocity field

[Ref. *Berezhko and G. F. Krymskii, 1981; Earl, J. R. Jokipii, ApJL, 1988; Ostrowski A&A, 1990; Webb ApJ, 1989; Rieger, Universe, 2019]*

Relativistic outflow speeds and sufficient energetic seed particles is needed to overcome adiabatic cooling

Shear acceleration scenario in radio galaxies have been proposed to explain UHECRs *[Kimura, Murase, BTZ, PRD, 2017; Seo et. al., ApJ, 2023]*

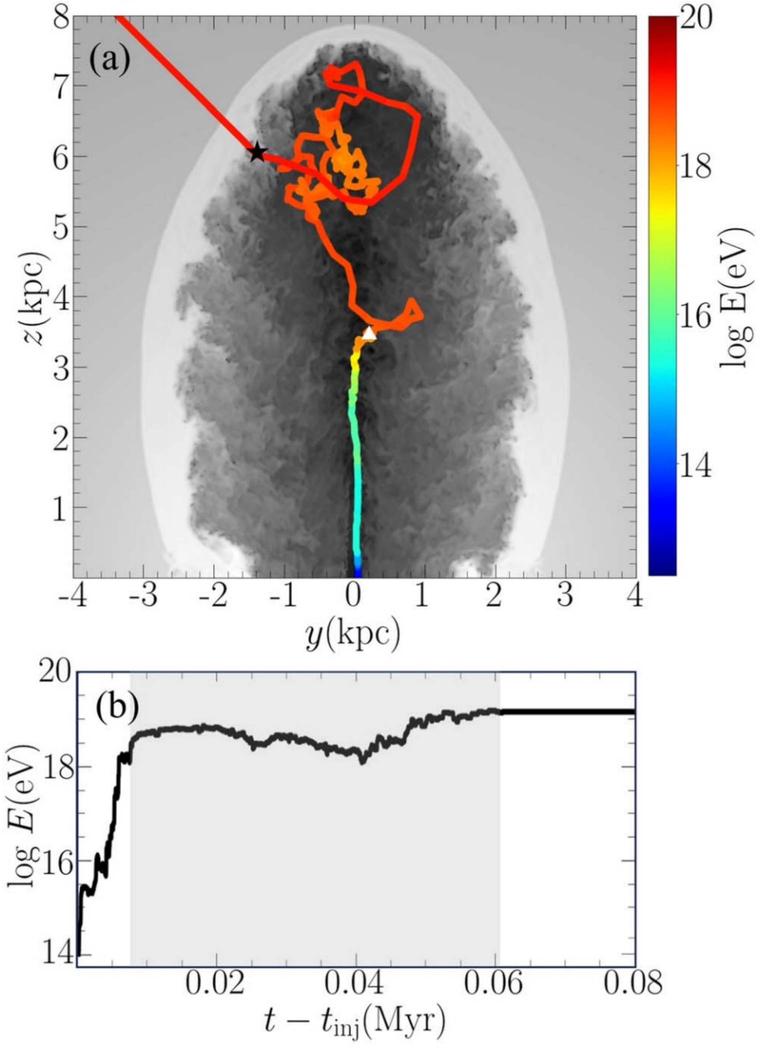

[Seo et. al., ApJ, 2023]

Diffusive shock acceleration in jets or wind termination shock is also possible

[Perettil et. al., 2025; Wang et al. 2025]

Energy spectrum from Shear acceleration

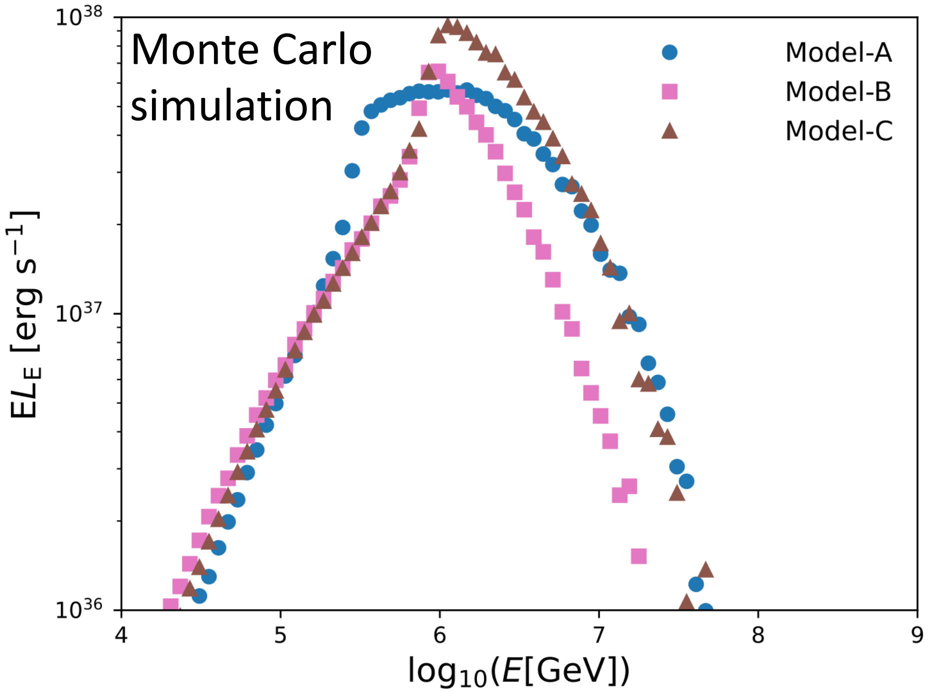

[Zhang, Kimura & Murase, 2026, PRD]

Model	$r_{\rm jet}$ [pc]	$B_{\rm jet}$ [μG]	$\beta_{\rm jet}$	$r_{\rm coc}$ [pc]	$B_{\rm coc}$ [μG]	$l_{\rm coh}$ [pc]	$l_{\rm jet}$ [pc]
A (default)	4	50	0.2	60	20	1.8	100
B	3	50	0.3	60	10	1.8	100
C	3	100	0.4	60	30	12	100

The escaping CR proton spectrum shows a hard component below the peak energy and a gradual cutoff above it

Balancing the acceleration and effective confinement timescales, the peak energy in the energy spectrum of escaping CR protons can be estimated to be:

$$t_{\rm conf} = \zeta_c R_{\rm jet}/c \ \sim \ t_{\rm acc} = \zeta_a \lambda_{\rm coc}/c\Gamma_{\rm jet}^2 \beta_{\rm jet}^2$$

$$E_{\rm max} = \zeta e B_{\rm coc} l_{\rm coh}^{1/2} r_{\rm jet}^{1/2} \Gamma_{\rm jet}\beta_{\rm jet} \simeq 4.3\ {\rm PeV} \left(\frac{B_{\rm coc}}{10\mu{\rm G}}\right) \left(\frac{l_{\rm coh}}{1.8\ {\rm pc}}\right)^{1/2} \left(\frac{r_{\rm jet}}{3{\rm pc}}\right)^{1/2} \left(\frac{\beta_{\rm jet}}{0.3}\right) \zeta$$

Compare to observed proton spectrum

[Zhang, Kimura & Murase, 2026, PRD]

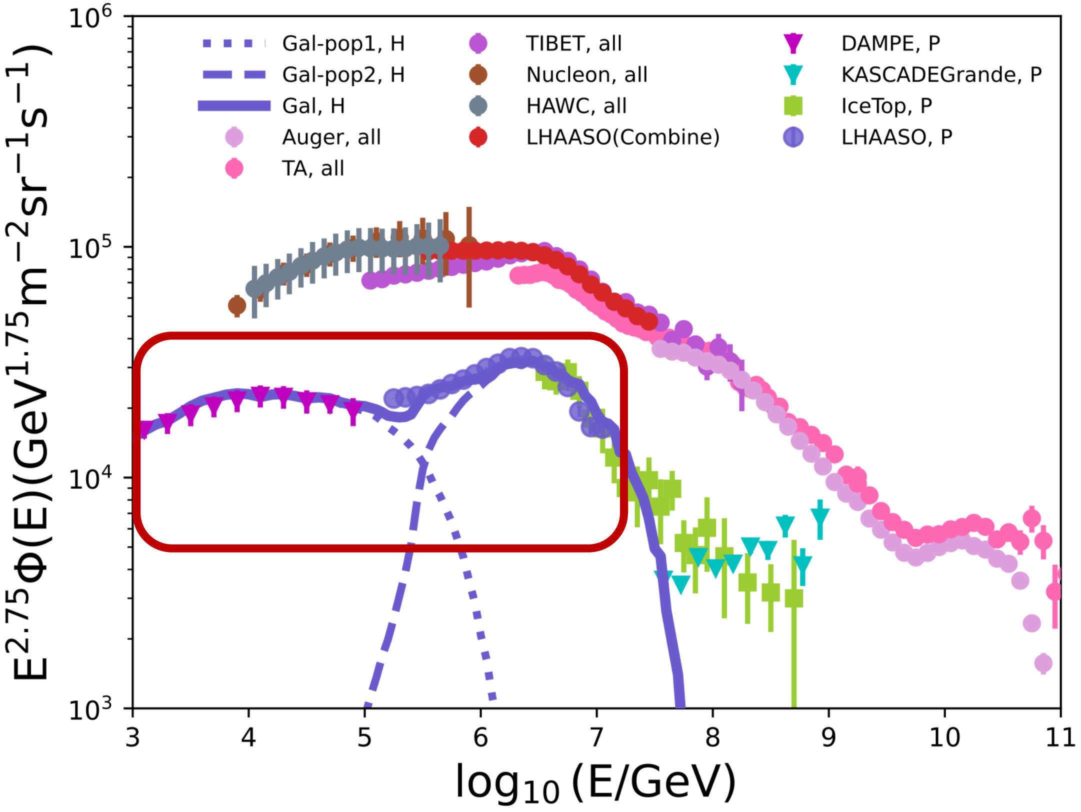

CRs from microquasars could explain both proton and all-particle spectrum around knee

The energy injection rate integrated over the Galactic volume:

$$L_{\rm cr,tot} = Q_{\rm CR,tot} V_G$$
$$\simeq 1.5 \times 10^{38}\ \mathrm{erg\ s^{-1}}$$

Consistent with the value required to explain CRs in the knee energy range if we have around 3-10 microquasars with extended jets in our Galaxy

Cosmic rays from mciroquasars

However, microquasars are characterized by lower spatial densities, the local CR flux is inherently subject to stochastic fluctuations …

Cosmic ray clouds from microquasars in our galaxy

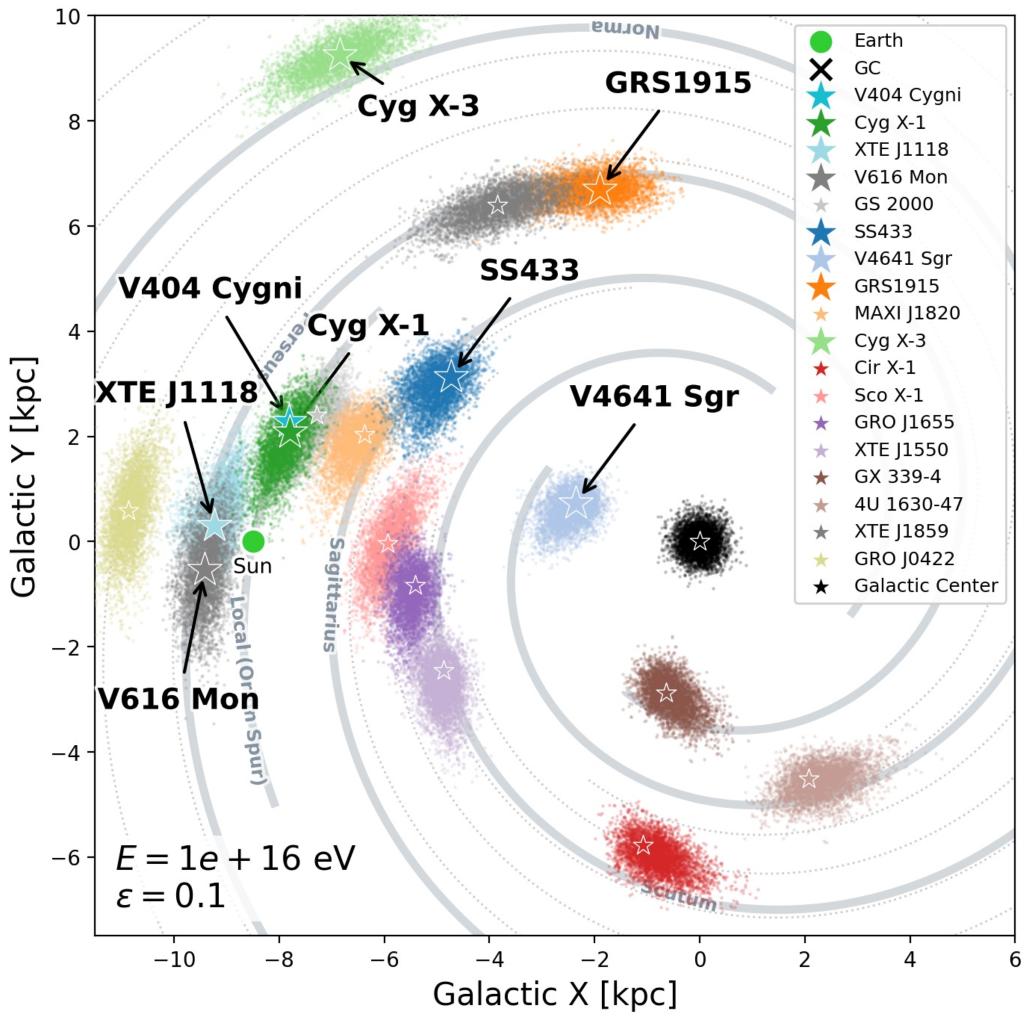

- llustration of the spatial distribution of 1 PeV cosmic rays (colored dots) from known Galactic microquasar locations (stars)

- The CR transport is influenced by the filamentary morphology of the Galactic magnetic field (gray spirals)

We employ constant diffusion with parallel coefficient to the regular magnetic-field direction as

$$D_{\|} = 6.1 \times 10^{28} (E/4\ \mathrm{GeV})^{1/3}\ \mathrm{cm}^2\ \mathrm{s}^{-1} \quad D_{\perp} = \varepsilon D_{\|}$$

In anisotropic diffusion scenario, the existence of regular GMF can results $D_{\|} > D_{\perp}$

Studies based on Galactic CR grammage constraints suggest an estimated range of ~0.01-0.1 from moderate to stronger cases

[e.g., Giacinti et. al., 2017, AL-Zetoun et. al., 2020]

[Zhang & Yu, 2026, PRL under review]

Propagation of CRs from nearby microquasar locations

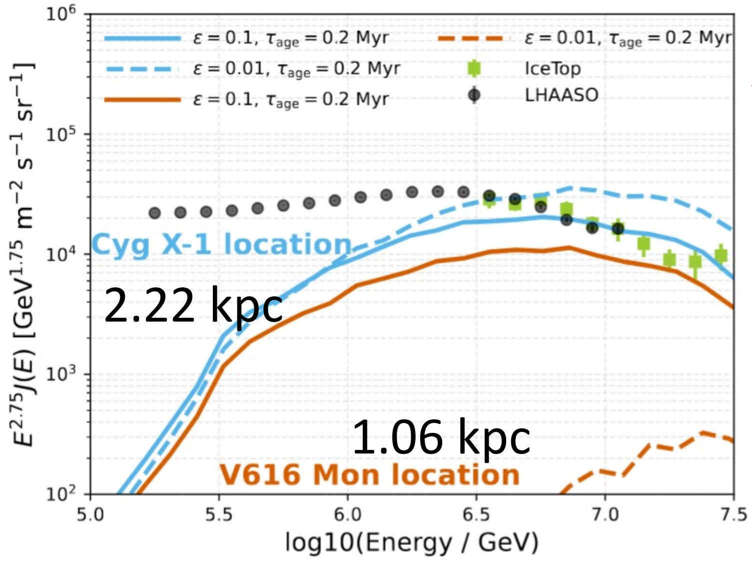

Active source scenario

CR flux observed on Earth after continuous injection of 0.2 Myr

For activate sources, the impact of the anisotropy diffusion parameter ε (dashed versus solid lines) is more significant than the physical distance of the source

$$Q = \eta_{\rm cr} L_{\rm Edd} \quad L_{\rm Edd} \simeq 1.26 \times 10^{39} (M_{\rm BH}/10\ M_\odot)\ {\rm erg\ s^{-1}}$$

CR acceleration efficiency $\eta_{\rm cr} \sim 0.5\%$

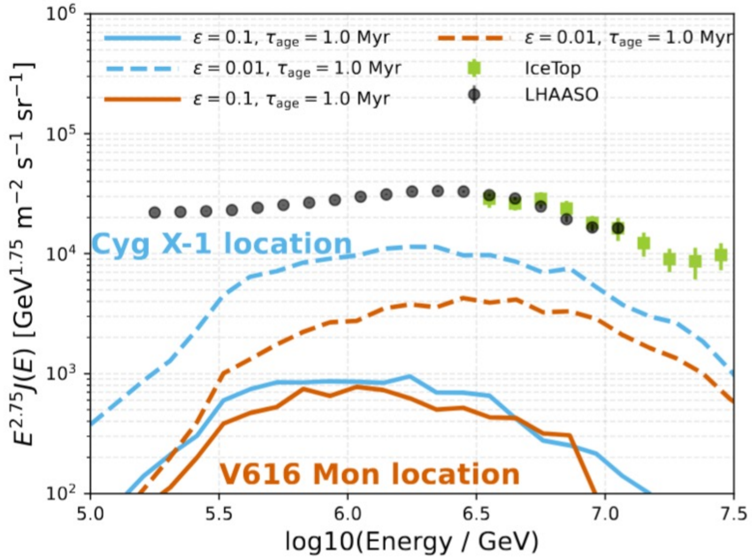

Remnant source Scenario

CR flux observed on Earth after 1 Myr, but the injection ceased up to 0.2 Myr

The active source exhibits a significantly harder spectral feature and a higher flux level

[Zhang & Yu, 2026, PRL under review]

CRPropa simulation

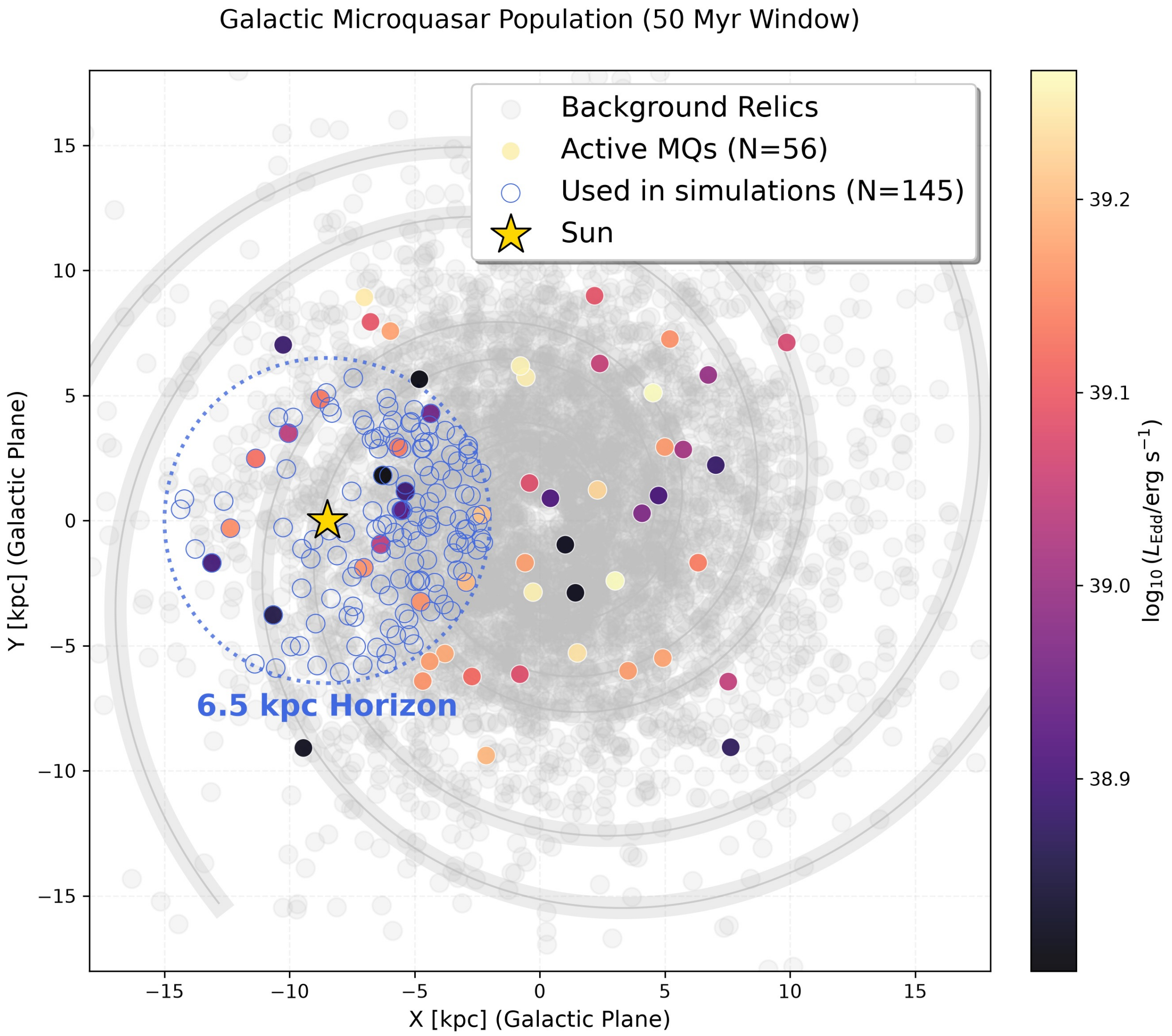

To account for spatial and temporal variance in the local microquasar population, we simulate an ensemble of 200 MC realizations using independent random seeds.

TABLE S2. Parameters used in the microquasar catalog generation and CRPropa simulation setup.

Parameter (Symbol)	Value / Distribution
Constants	
Birth Rate	1×10^{-4} yr^{-1}
CR Loading Efficiency ($\eta_{\rm cr}$)	0.1
Simulation Cutoff	6 Myr & non-active
Sample Ensembles	
Lookback Time ($t_{\rm lookback}$)	$\mathcal{U}(0, 50)$ Myr
Jet Duration ($t_{\rm duration}$)	$\mathcal{U}(0.1, 1.0)$ Myr
Black Hole Mass ($M_{\rm BH}$)	$\mathcal{U}(5, 15)\ M_\odot$
Galactocentric Radius ($r_{\rm gc}$)	Green15
Vertical Height ($z_{\rm gc}$)	$\pm$Exp($h_z = 0.15$ kpc)
CRPropa Simulation	
Injected Primary	protons
Energy Range	[100 TeV, 100 PeV]
Energy Bins	21 (log-spaced)
Particles per Bin	25,000

[Zhang & Yu, 2026, PRL under review]

Diffuse CR energy spectra

- Both can reproduce the bump while PL has nicer low-energy extension
- The PeV bump in the CR proton spectrum is robust rather than being an occasional outlier

Model A (hard): $\eta_{\rm cr} \sim 0.3 - 1.5\%$

PL with index = 2: $\eta_{\rm cr} \sim 2 - 10\%$

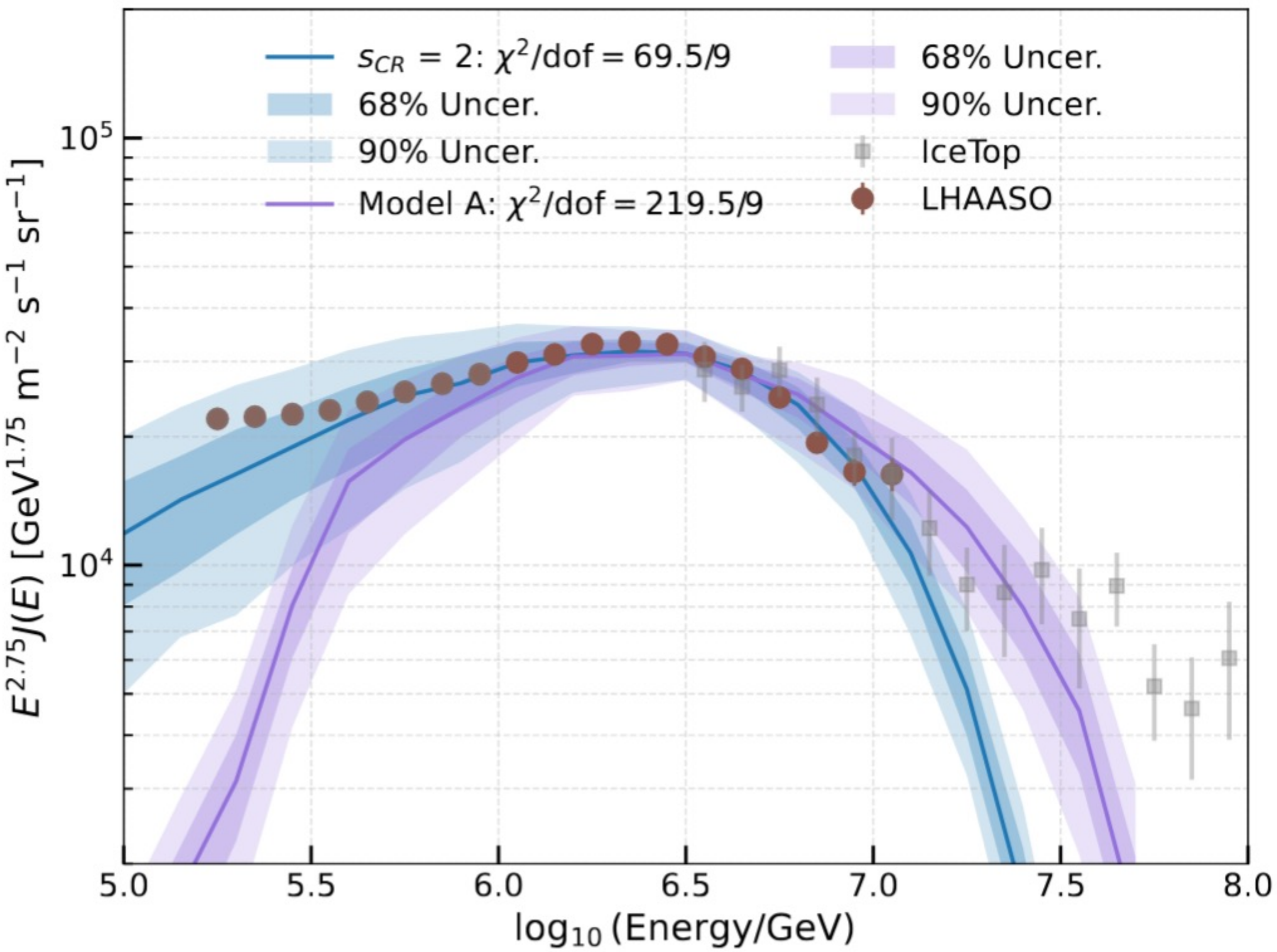

[Zhang & Yu, 2026, PRL under review]

Two realizations of source distributions

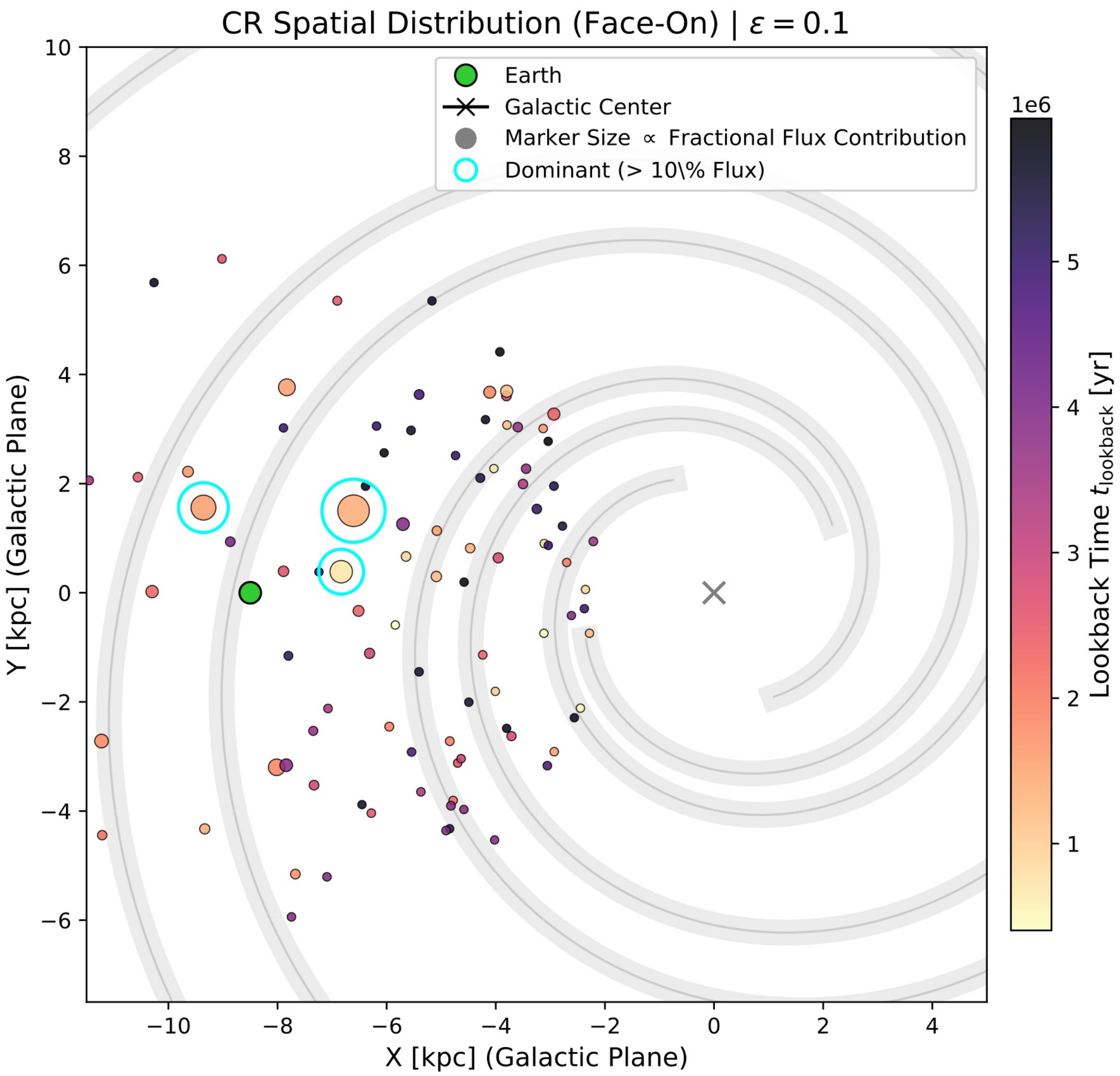

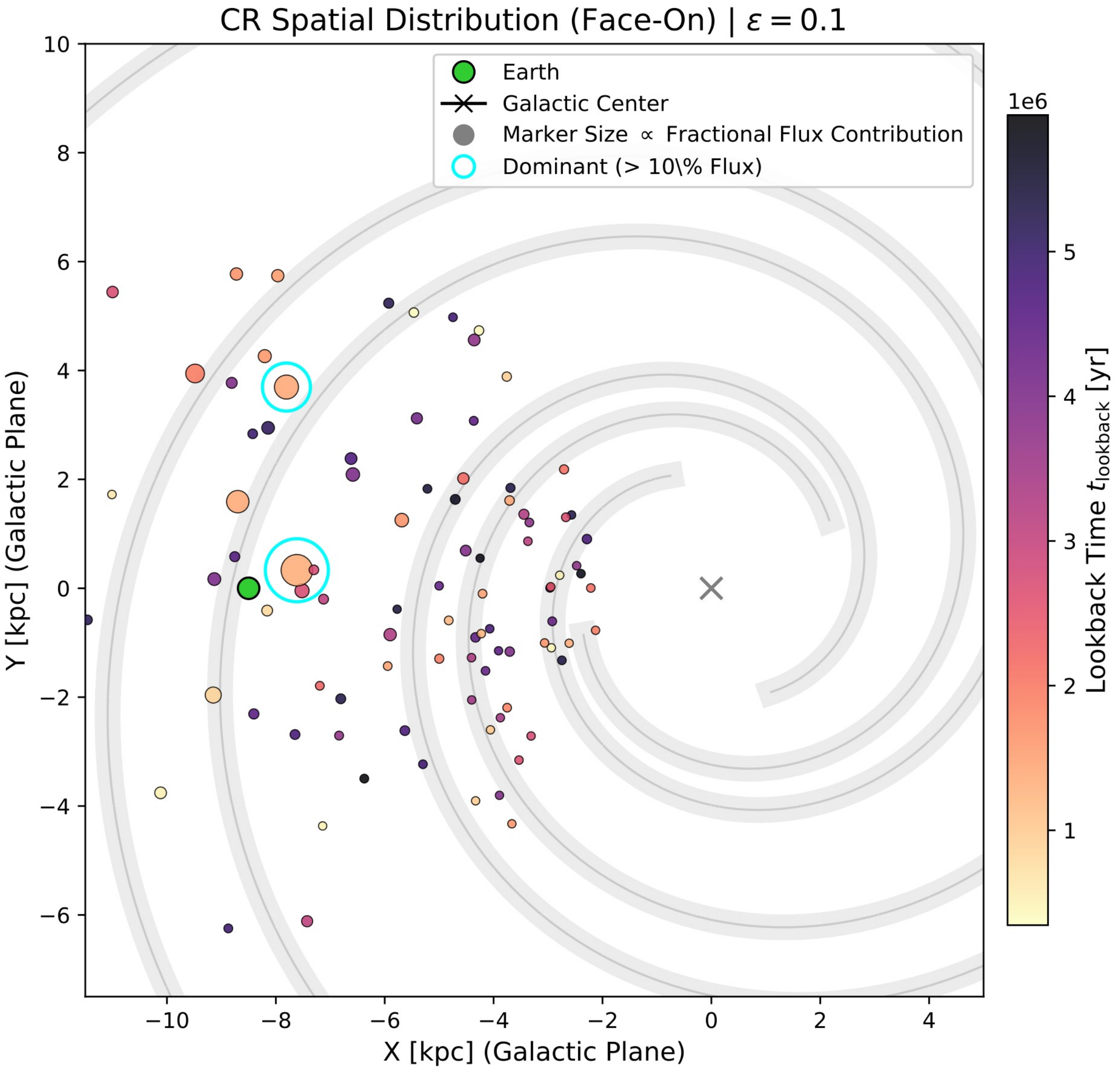

[Zhang & Yu, 2026, PRL under review]

Rank the fraction of flux from the individuals

We calculate and rank the fraction of flux contributed from the individuals in each ensemble

- Usually no more than four sources are needed to explain 50% of the observed flux at 1 PeV

- The top ~10 sources contribute ~80%

Therefore, the local PeV CR flux may not be a simple steady-state global average, but rather. dominated by a few recent and nearby microquasar remnants

[Zhang & Yu, 2026, PRL under review]

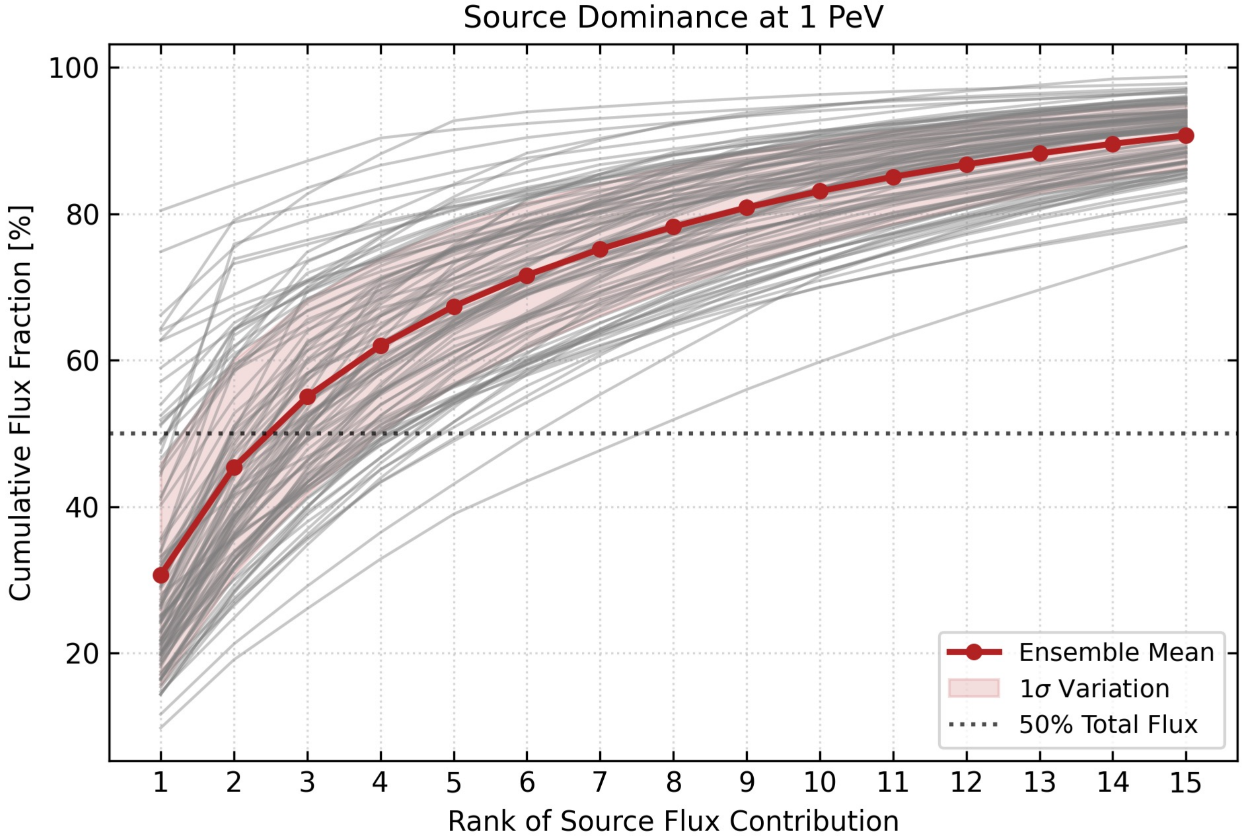

Cumulative fraction of the local CR flux at 1 PeV as a function of source rank, with sources ordered by their individual flux contributions

Effects of source radial distribution

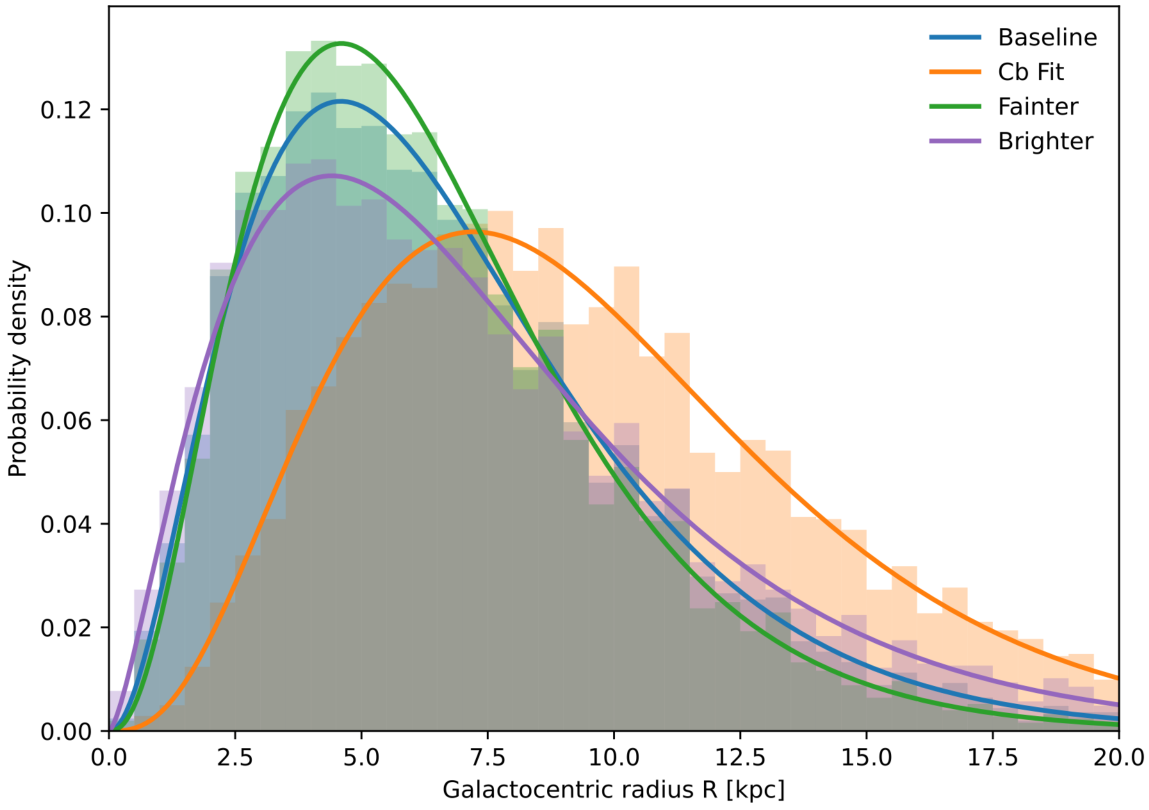

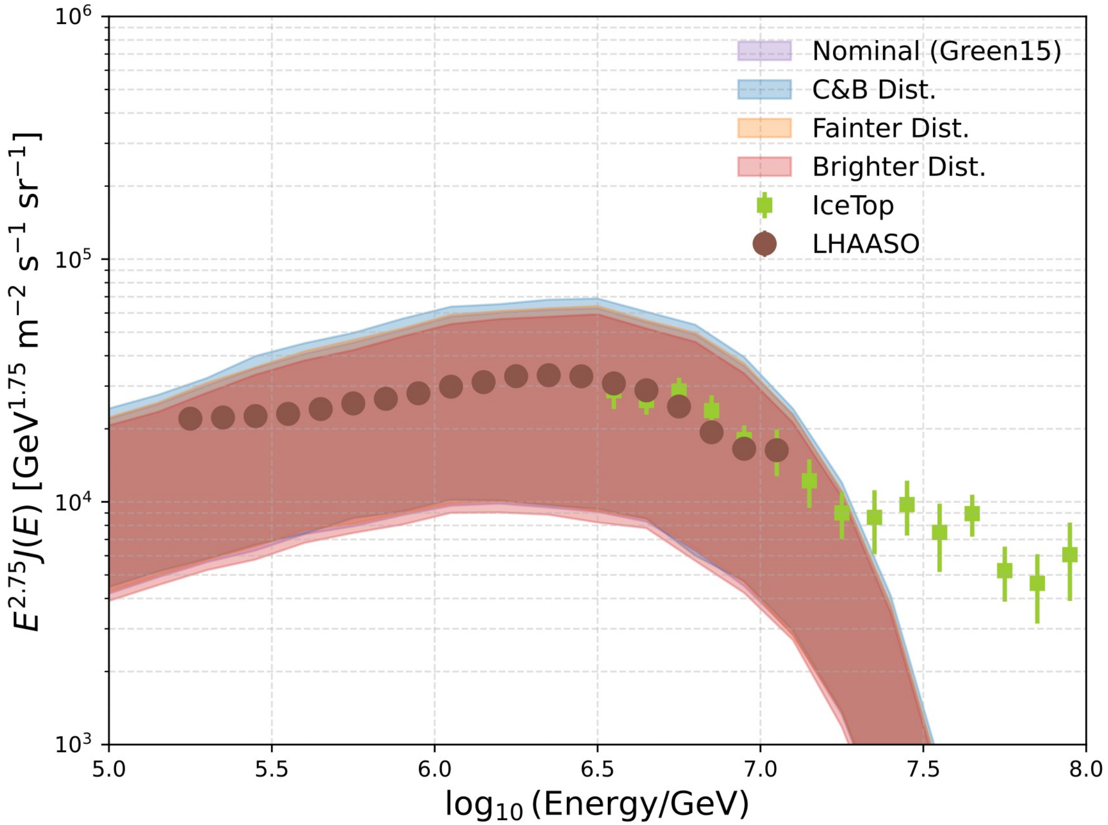

We test three more source distributions and show that their impacts on our predicted CR spectra is negligible

[Zhang & Yu, 2026, PRL under review]

Cosmic ray Composition

The composition of cosmic rays is the key

Proton to helium ratio

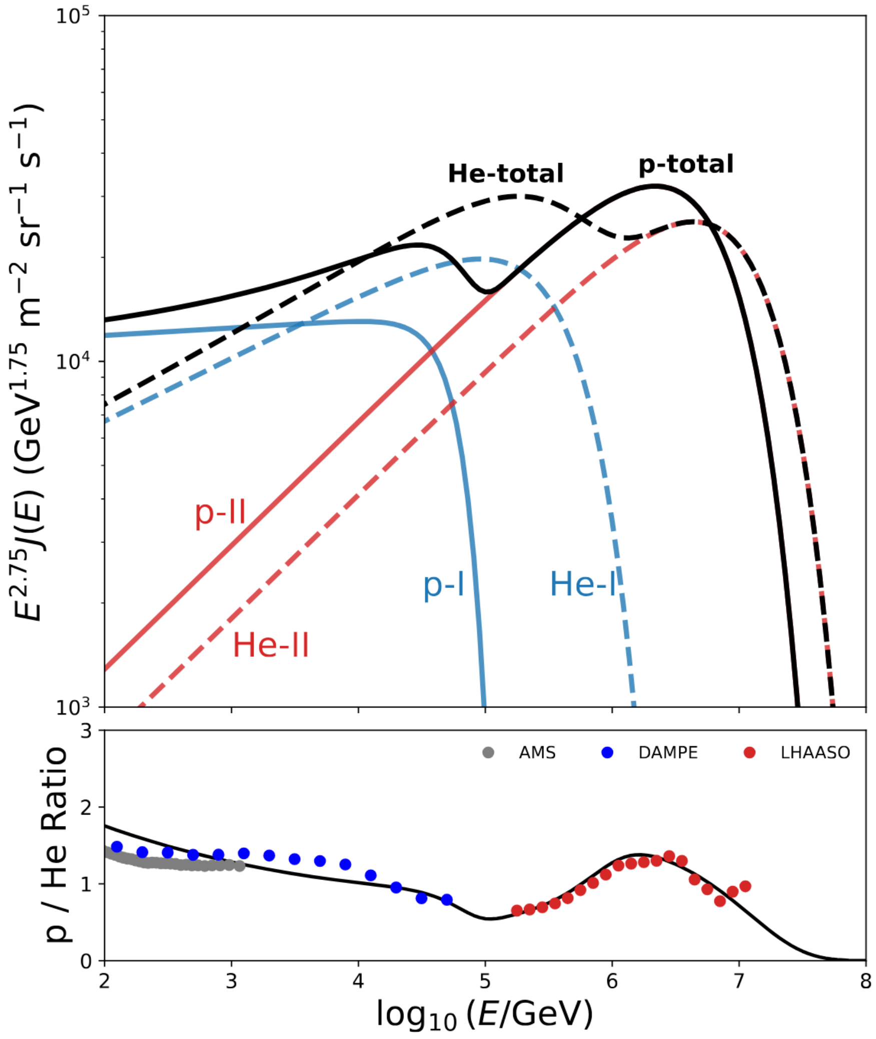

The differences between the proton and helium spectra provide a natural explanation for the behavior of the p/He ratio

The decrease and subsequent recovery in the multi-TeV region arise from the transition between the two components

The maximum in the p/He ratio at PeV energies can be understood as a consequence of the interplay between the two components and their different cutoff energies for protons and helium, e.g., earlier cutoff of the proton spectrum

[Aharonian and BTZ, 2026, ApJ]

Injected CR composition in five massive groups

	Z	A	Scenario 1: $f_{A,300\mathrm{GV}}$	Scenario 1: $f_{A,100\mathrm{GV}}$	Scenario 1: $f_{A,1\mathrm{TV}}$	Scenario 2: $f_{\odot}$	Scenario 3: $f_{\odot}^{\mathrm{enhance}}$
P	1	1	0.787	0.803	0.767	0.922	0.747
He	2	4	0.194	0.18	0.212	0.077	0.250
CNO	7	16	0.0145	0.013	0.0157	0.007	0.003
NeMgAlSi	12	28	0.00374	0.00352	0.004	0.001	0.0006
Fe	26	56	0.00121	0.00097	0.0014	0.00002	0.0001

TABLE II. Injected CR composition at the rigidity 300 GV, 100 GV, and 1 TV for different composition models. In addition, we also include solar composition $f_{\odot}$ and enhanced solar composition $f_{\odot}^{\mathrm{enhance}}$ by a factor of $(A/Z)^2$.

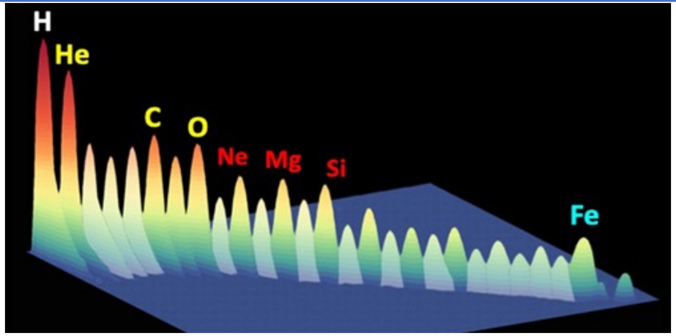

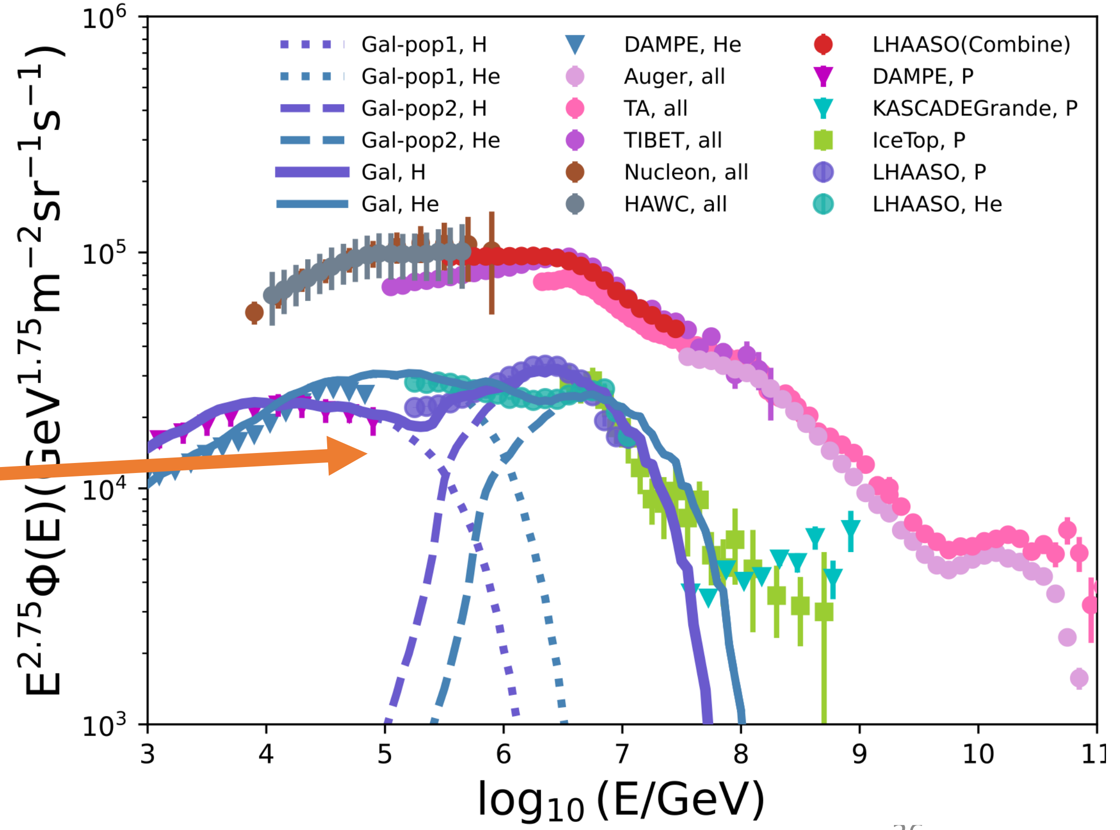

- CR composition ratio at the same rigidity: 300 GV, 100 GV and 1 TV
- CR composition ratio same as solar system abundance
- CR composition ratio same as solar system abundance with enhancement by a factor of (A/Z)^2

[Zhang, Kimura & Murase, 2026, PRD]

Observed CR spectrum and composition on Earth

Our analysis shows that reaccelerating low-energy CRs (100 GV– 1 TV) yields a mean logarithmic mass roughly consistent with observations near the CR knee

Models assuming solar or enhanced solar compositions fail to reproduce the observed mass distribution.

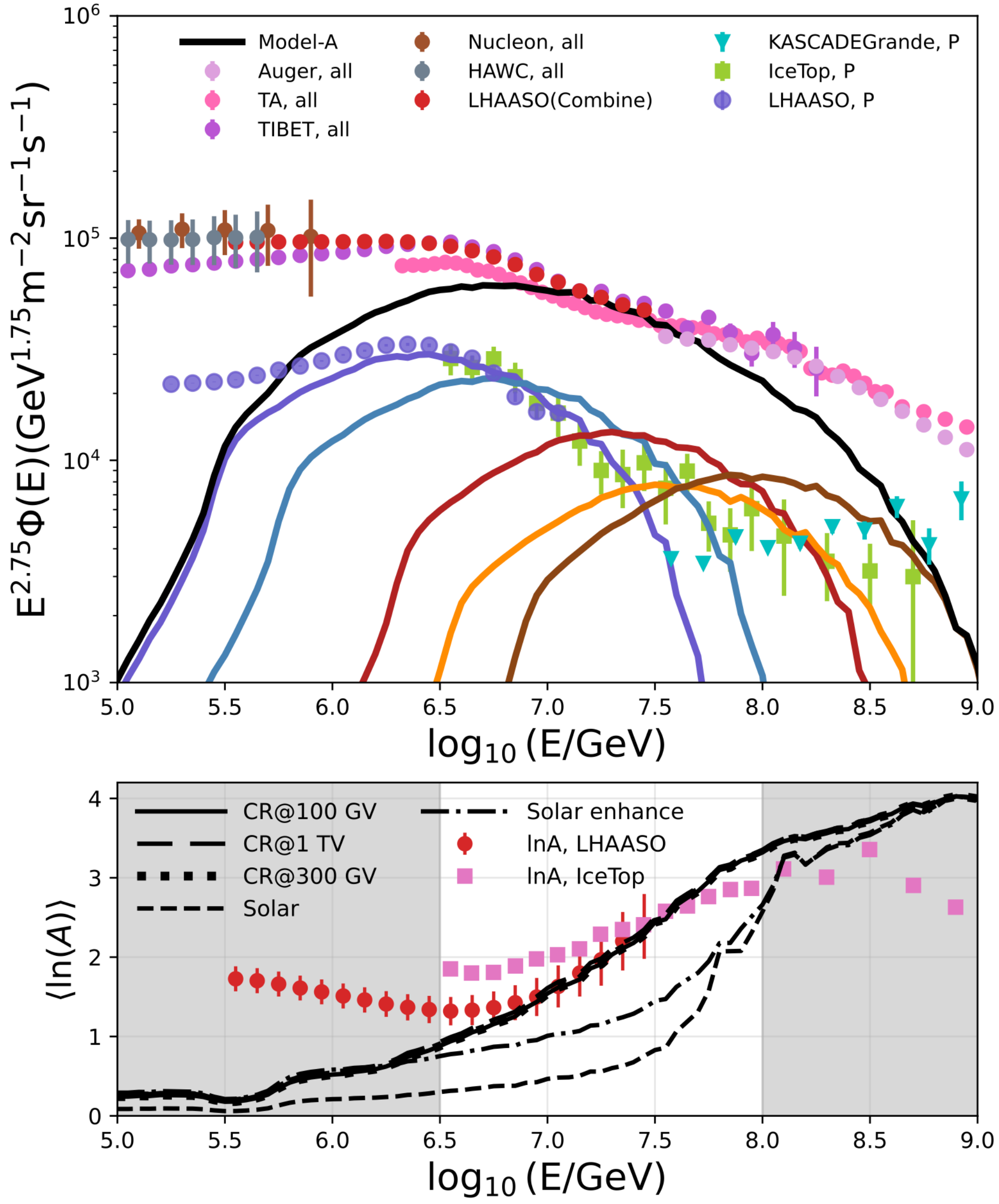

[Zhang, Kimura & Murase, 2026, PRD]

Reacceleration model in microquasars and radio galaxies

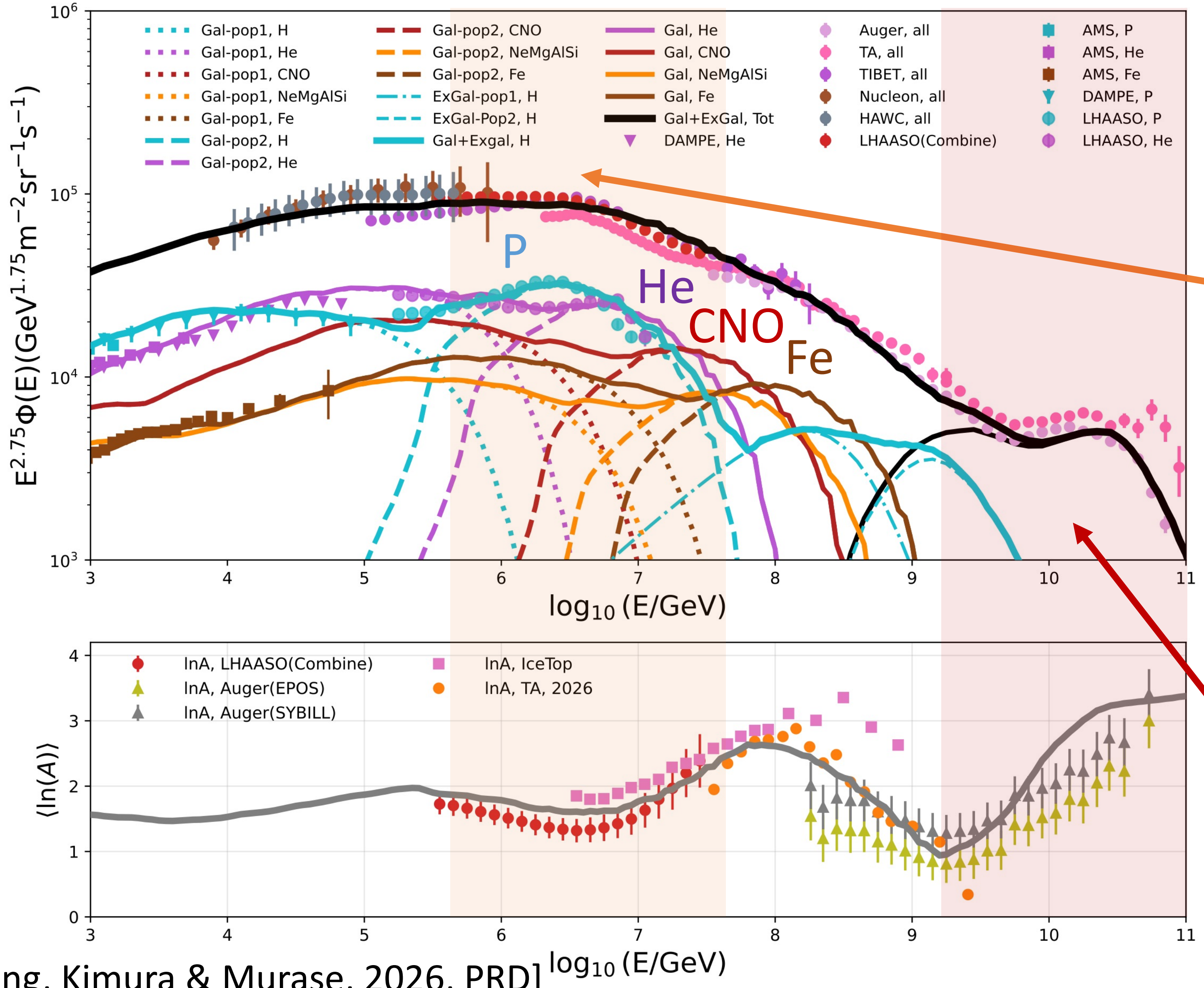

[Zhang, Kimura & Murase, 2026, PRD]

The reacceleration model works not only in the microquasars but also in the large-scale jet-cocoon system in radio galaxies

Gal pop2: CRs from microquasars (MQ)

Shear acceleration

Re-acceleration around 300 GV

[Ref. BTZ , Kimura, Murase, 2025]

The model is testable by LHAASO's CNO and Fe measurement

ExGal pop2: UHECRs from radio galaxies (RG)

Shear acceleration

Re-acceleration around 1 TV

[Ref. Kimura, Murase, BTZ, 2018]

Galactic diffuse neutrinos and gamma-rays

- Secondary gamma-rays and neutrinos are produced from hadronic (*pp*) interactions between CRs with ambient gas

- CR fit results yield a Solar neighborhood average, likely would miss the Galactic-level fluctuations can be traced by neutrinos and gamma rays → need multi-messenger constraints.

Galactic diffuse VHE gamma-ray and neutrino emission

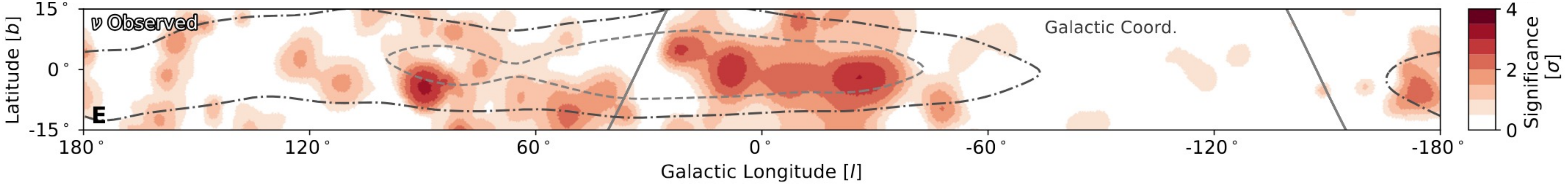

- Gamma-rays (diffuse + unresolved src including leptonic process) v.s. neutrinos (diffuse + all src)

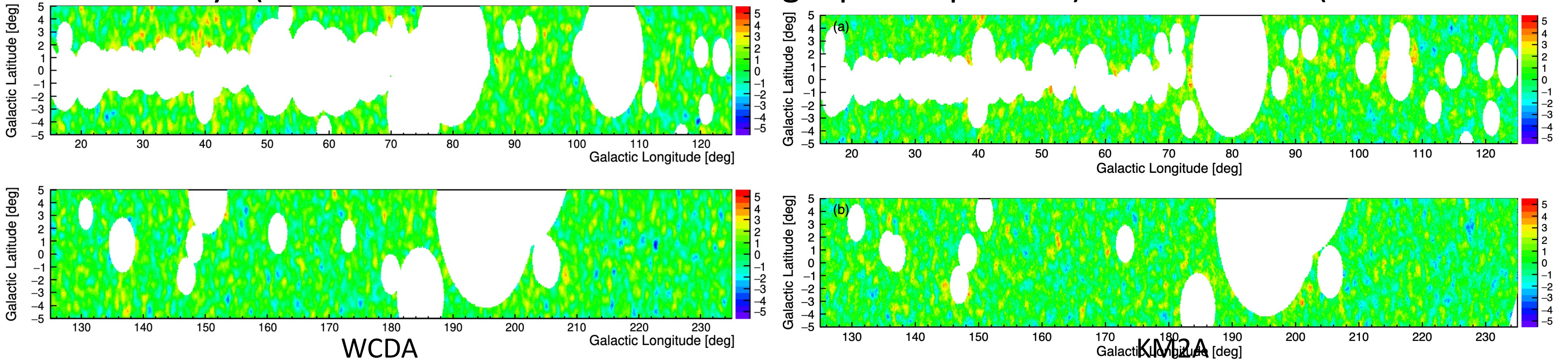

- CRs observed at Earth mainly from nearby sources, while diffuse gamma rays and neutrinos needs to account for sources across the whole galaxy

[Yu & BTZ, 2026, submitted to ApJL] [*See the talk in the afternoon*]

Summary and outlook

第二课题组目前已经发表文章14篇，另有5篇审稿中，已完成预定年度计划。

课题二指标：宇宙线“膝区”结构成因理论模型

- ✓ 围绕银河系宇宙线的起源与传播开展了一系列系统性研究，重点探讨了超新星遗迹和微类星体在银河系宇宙线不同能段中的贡献，分别对低能端和高能端宇宙线能谱进行了统一解释

下一步计划：

- ✓ 结合银河系磁场模型，构建考虑各向异性扩散和空间依赖效应的宇宙线传播模型，重点研究宇宙线成分演化、大尺度各向异性的形成机制以及银河系宇宙线向河外宇宙线过渡的物理过程

- ✓ 在已有超新星遗迹和微类星体研究的基础上，进一步拓展银河系宇宙线源的研究范围，研究脉冲星风云、恒星形成区等天体中的宇宙线加速、逃逸及其辐射机制

Backup

Origin of the knee – Propagation effect?

- Cosmic ray propagation inside galaxy

e.g., *Syrovatsky (1971), Ptuskin (1992), Giacinti (2014,2015)*

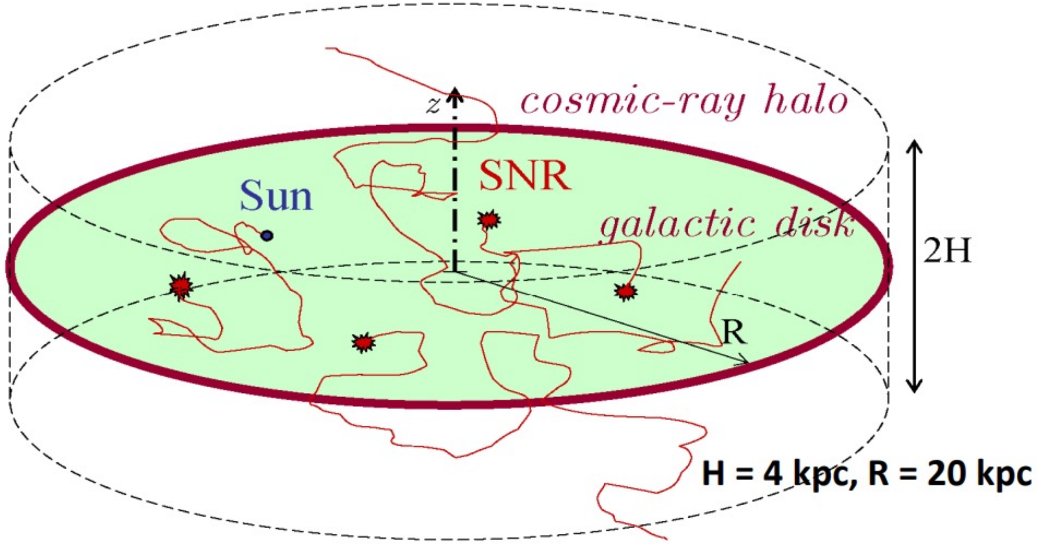

Constant diffusion coefficient

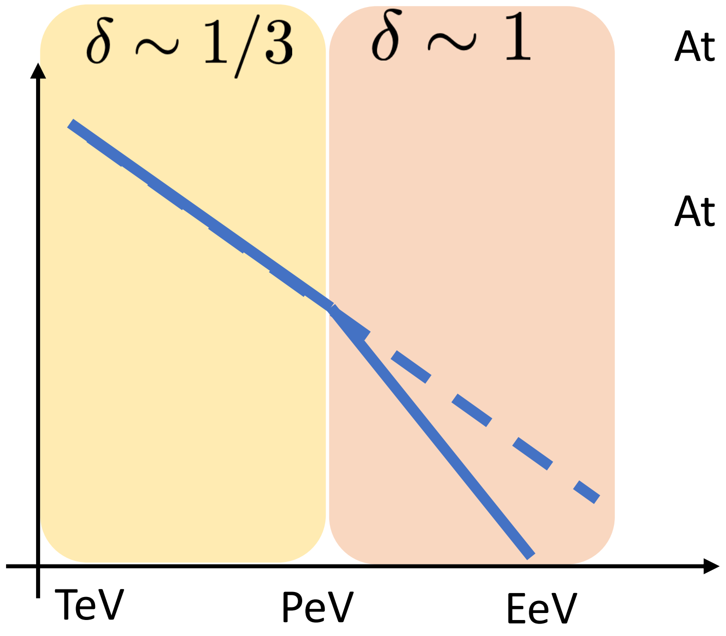

At Source:

$$\mathcal{R}^2 dN/d\mathcal{R} \propto \mathcal{R}^{2-s_{\rm sec}}$$

At Earth:

$$\mathcal{R}^2 \Phi_{\mathcal{R}} \propto (\mathcal{R}^2 dN/d\mathcal{R}) X_{\rm esc}$$
$$\propto \mathcal{R}^{2-s_{\rm esc}-\delta}$$

The grammage traversed by CRs during propagation $X_{\rm esc} \simeq \mathcal{R}^{-\delta}$

A physically motivated overall picture of CRs

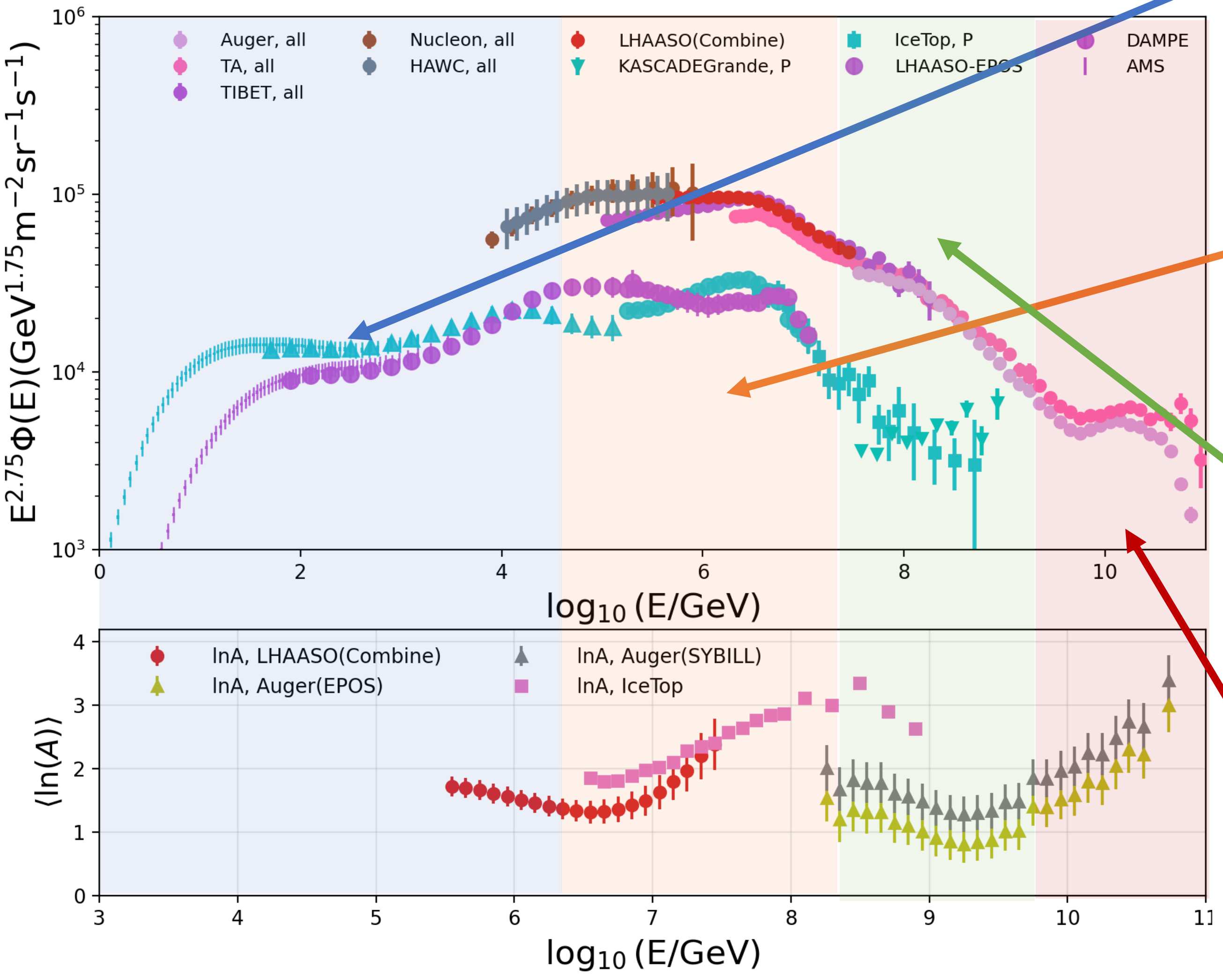

Gal pop1: CRs from supernova remnants (SNR)

Gal pop2: CRs from microquasars (MQ)

Or other Galactic PeVatrons?

Or Gal pop3: Galatic powerful sources?

ExGal pop1: CRs from extra-galactic sources: e.g, clusters of galaxies or nearby AGN

ExGal pop2: UHECRs from radio galaxies (RG)

Or other sources, e.g., GRB, TDE, ?

第二课题：研究进展

其他

- Qian, Sun, Nie, Ge, Liu & Guo, Monogem’s Contribution to the Galactic Cosmic-Ray Spectrum, ApJ , 2025
- Qiao, Liu, Yan & Guo, The Compton-Getting origin of the large-scale anisotropy of Galactic cosmic rays, ApJ, 2025

Galactic proton and helium spectum

Proton and helium spectrum measured from LHAASO

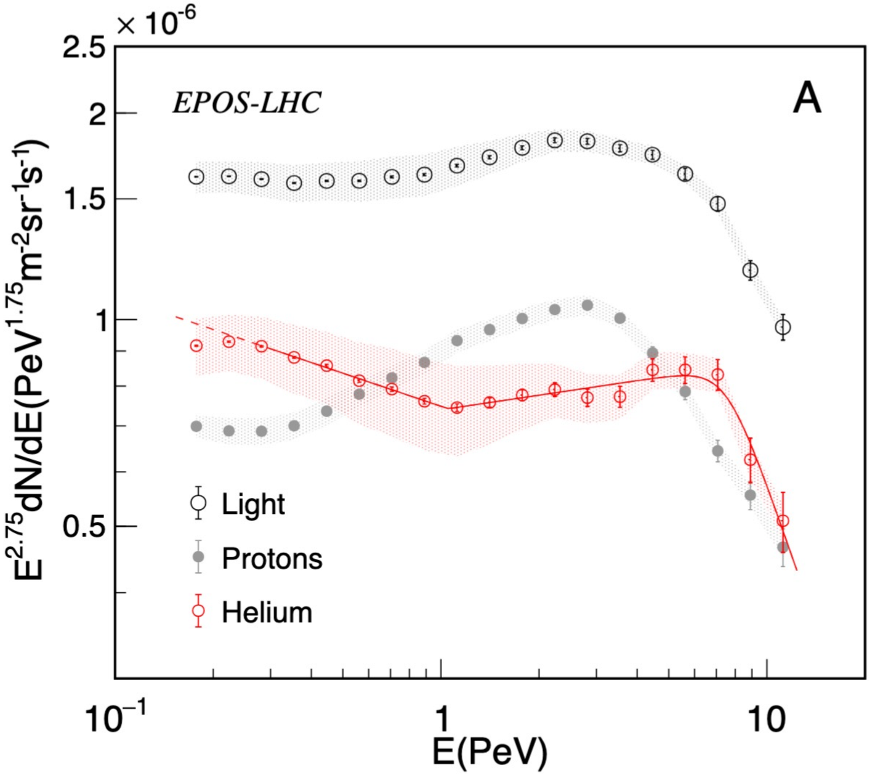

[LHAASO Collaboration, 2026, PRL, arXiv: 2511.05013]

[See also, LHAASO Collaboration, 2025, Sci. Bull. arXiv: 2505.14447]

An event measured by KM2A ED array (A) and a Cherenkov telescope of WFCTA (B)

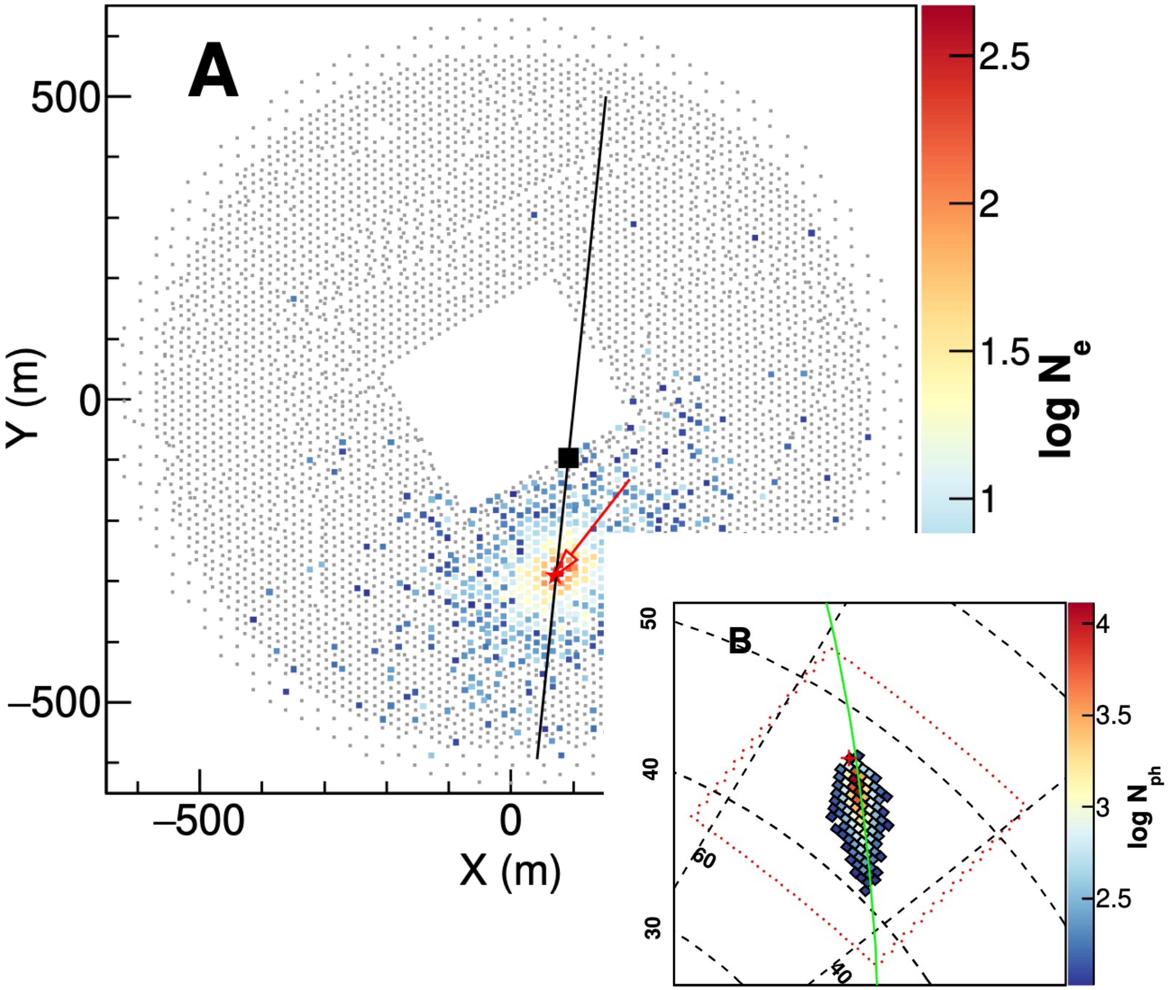

Implications of LHAASO results

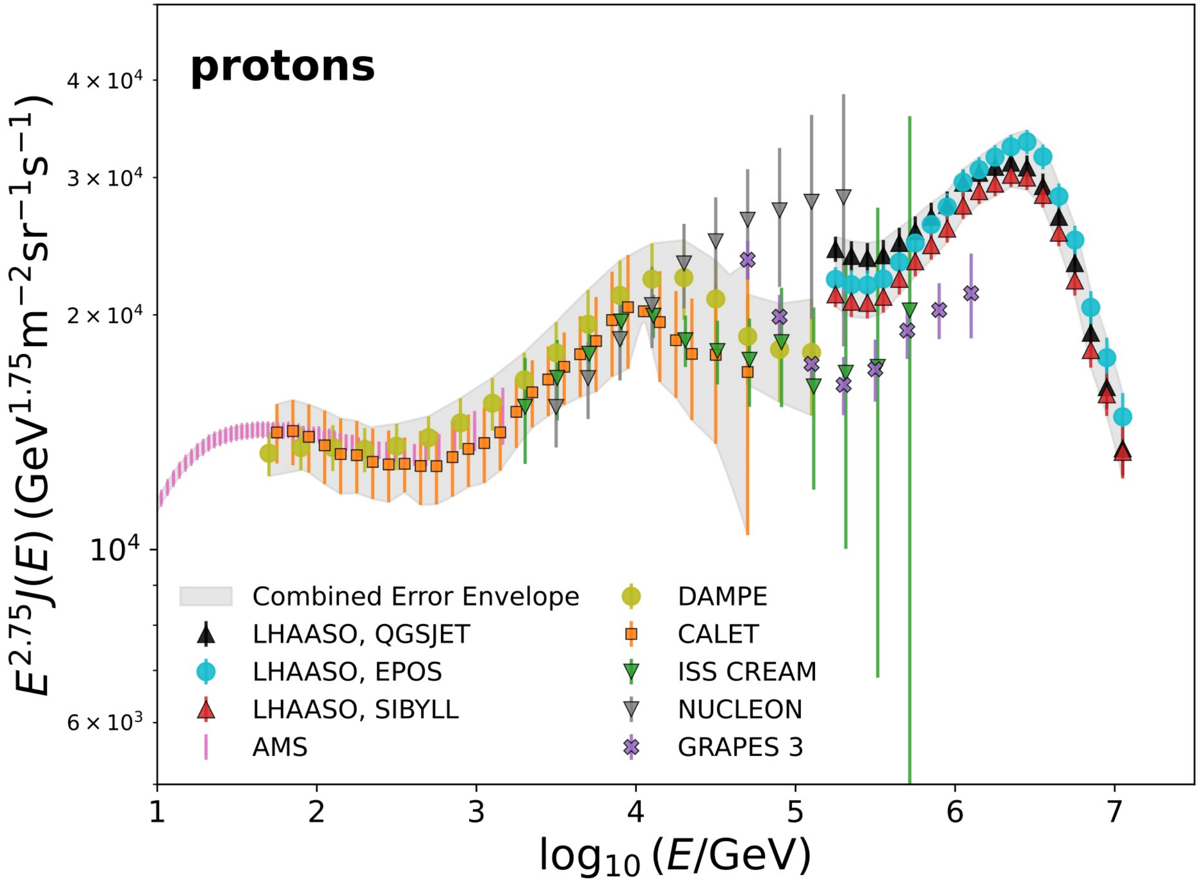

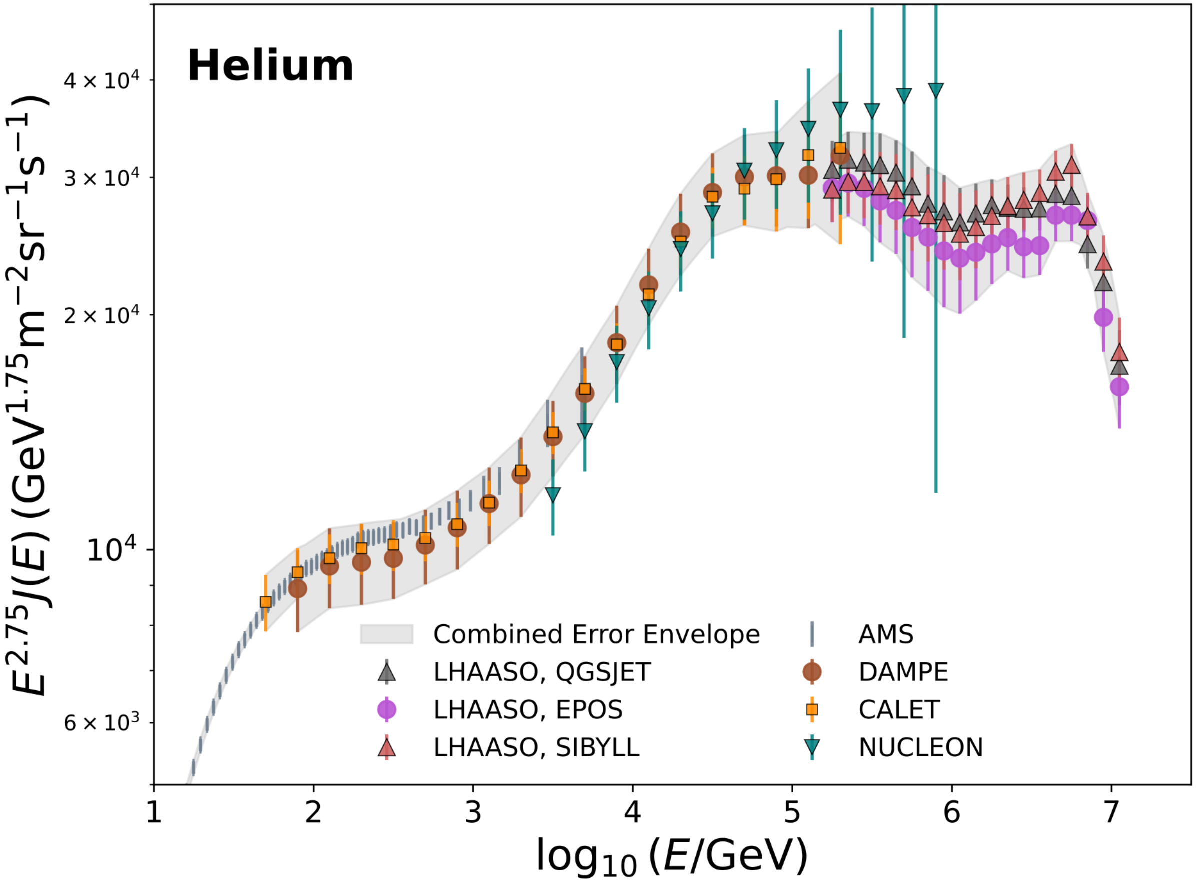

- LHAASO reported the high-purity proton spectrum, implicating the knee at the energy around 3 PeV is related to the change of the proton spectrum

- The observed hardening feature above several hundreds of TeV implicates the emergence of a new source component that has the maximum energy at least up to a few PeV

Galactic PeVatrons and the second CR component

- Old SNRs as smoking UHE gamma-ray guns （特殊的超新星遗迹）

  A subset of SNRs operates as proton PeVatrons and contributes non-negligibly to the second CR component - e.g., higher shock velocity; magnetic field amplification

  Absence of UHE γ-ray detections from young SNRs -> Disfavor SNRs as PeVatrons? E.g. Cas A

  Escaped CRs interact with nearby giant molecular cloud – “smoking gun”

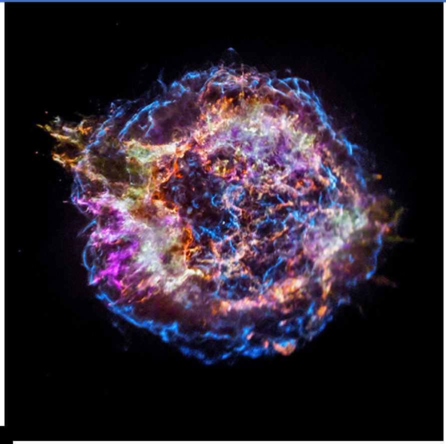

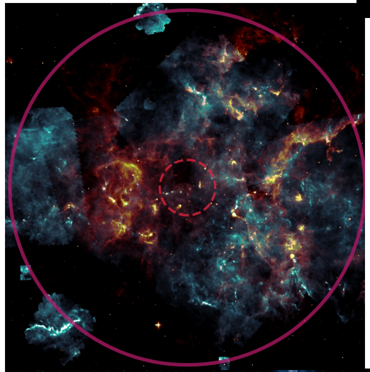

- Star-forming regions as sites of proton PeVatrons （恒星形成区）

  Cygnus OB2

  Detailed theoretical studies indicate that reaching the PeV domain through stellar-wind interactions alone is highly challenging

  Or supernovae occurring within stellar clusters may play a dominant role?

- Microquasars as Galactic PeVatrons

  （微类星体时银河系拍电子伏加速源）

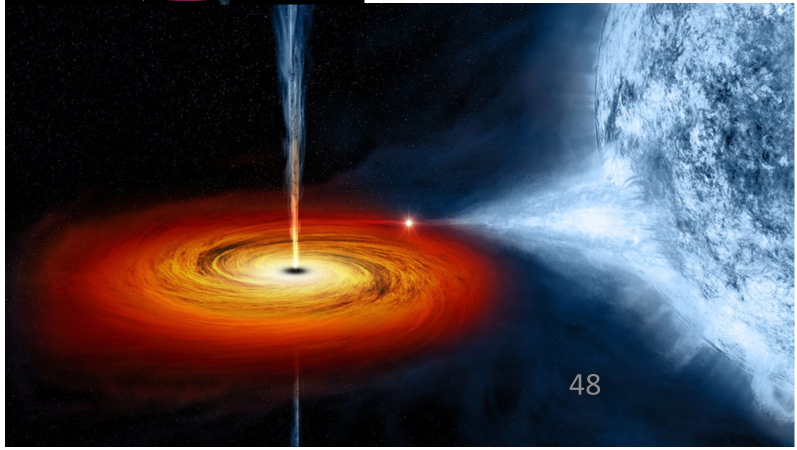

Microquasar – SS 433

The extended two-sided jets with ~ 40 pc are detected in X-rays

Radio lobes surrounding the system extends up to ~ 150 pc

VHE gamma-ray emission from SS 433 has been detected at the jet lobes, which are spatially co-incident with the X-ray hotspots

LHAASO Coll, NSR, 2025

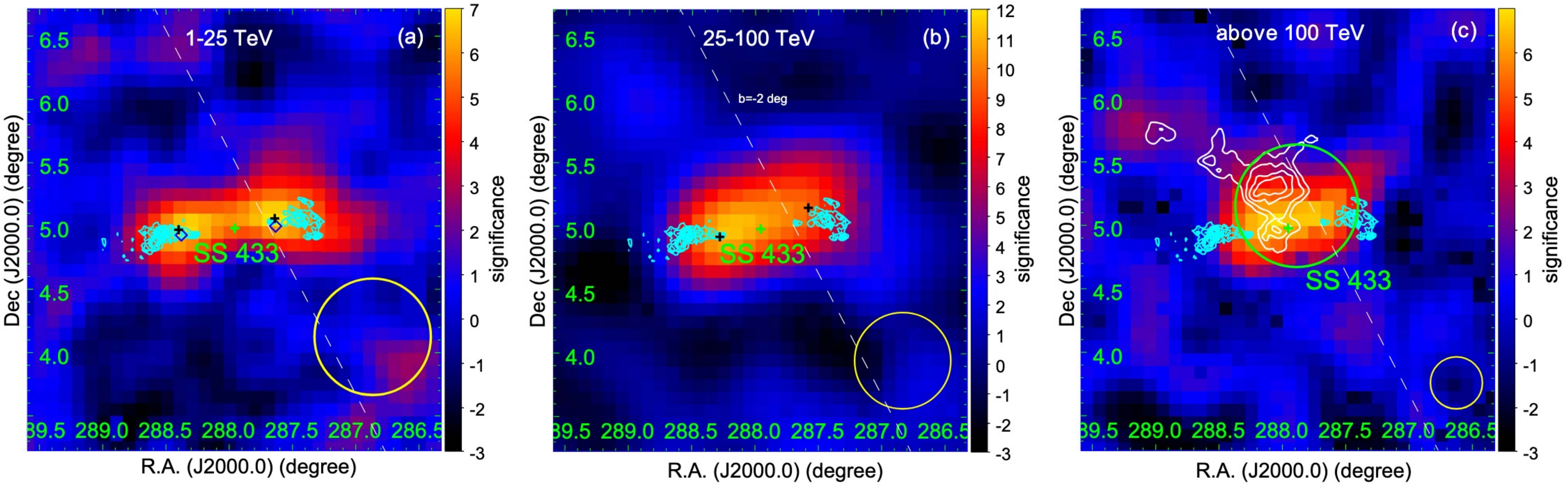

Microquasar – V4641 Sgr

V4641 Sgr is another interesting microquasar who emits gamma-rays above 100 TeV

The morophorogy of the gamma-ray signal is clear two-sided lobe structure, and the size of the lobe is roughly ~ 100 pc

Spatially extended X-ray signature is also detected

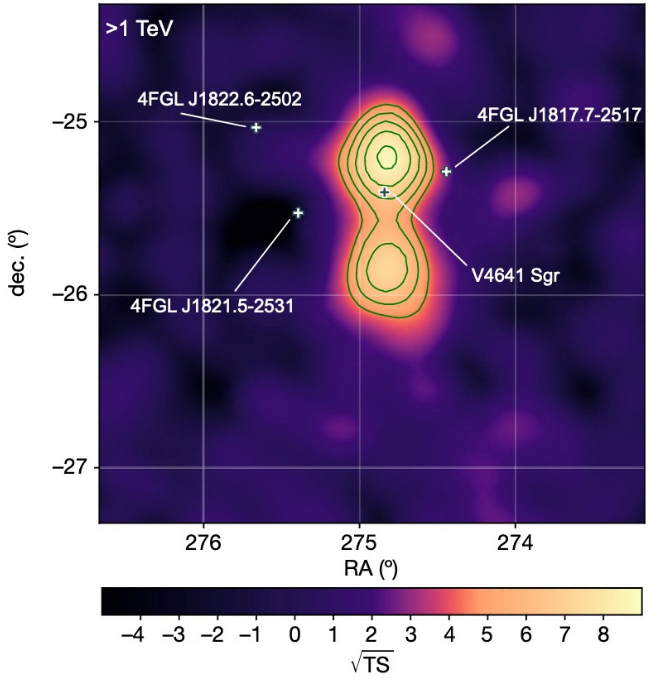

HAWC Coll, Nature, 2024

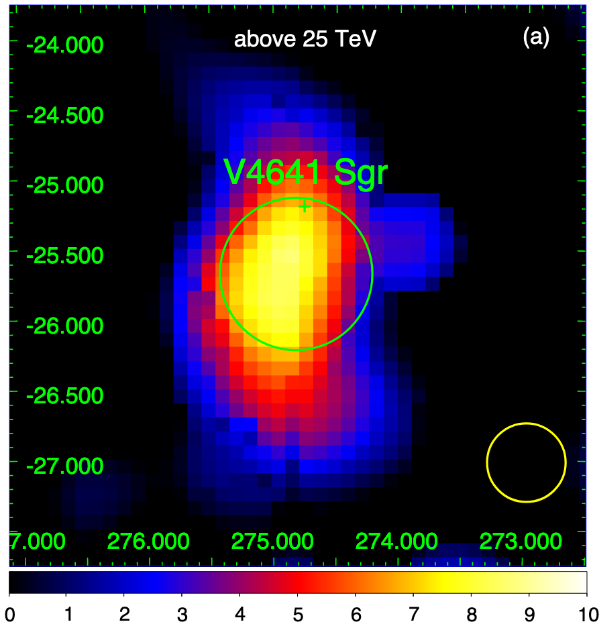

LHAASO Coll, NSR, 2025

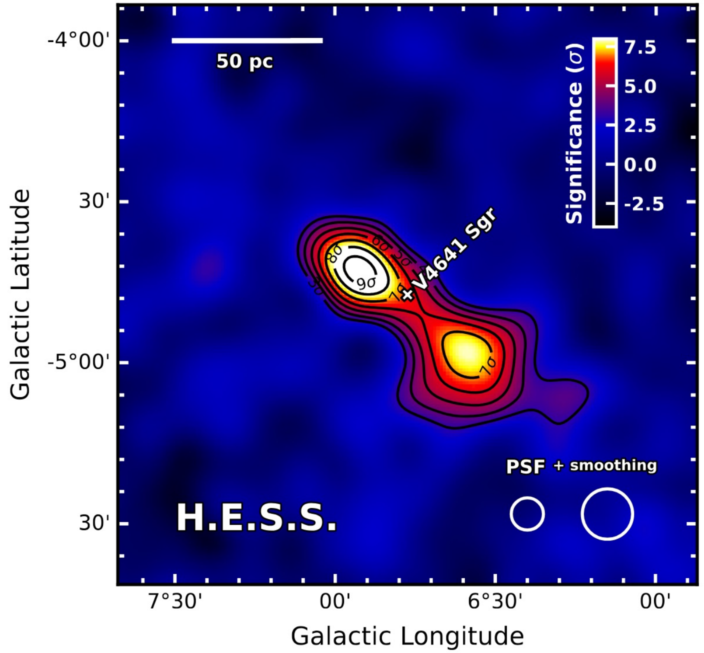

HESS Coll, A&A, 2025

GRS 1915+105 – large-scale jet and jet-driven bow shock

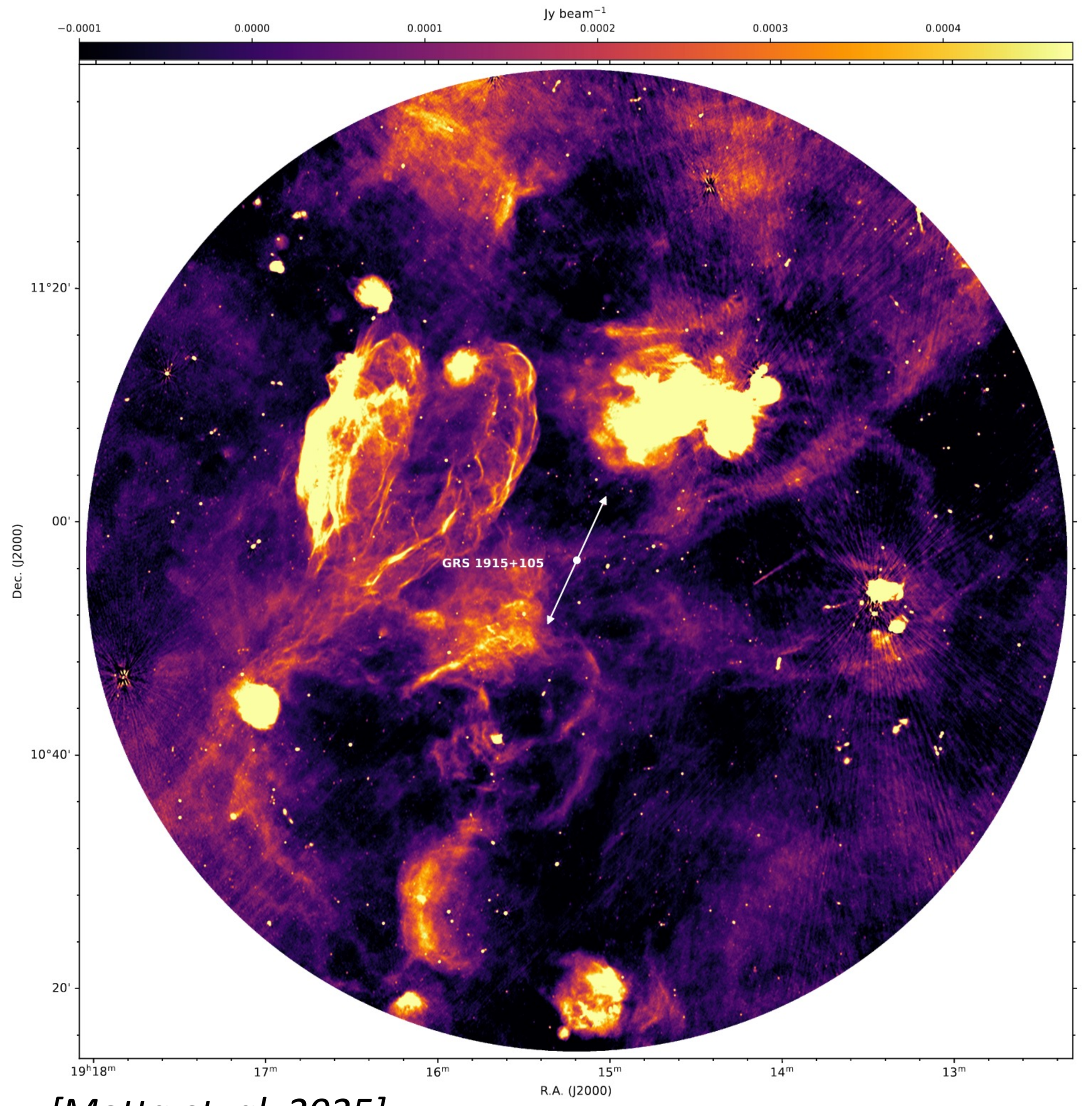

[Motta et. al. 2025]

Zoom-in of the jet–ISM interaction region by MeerKAT

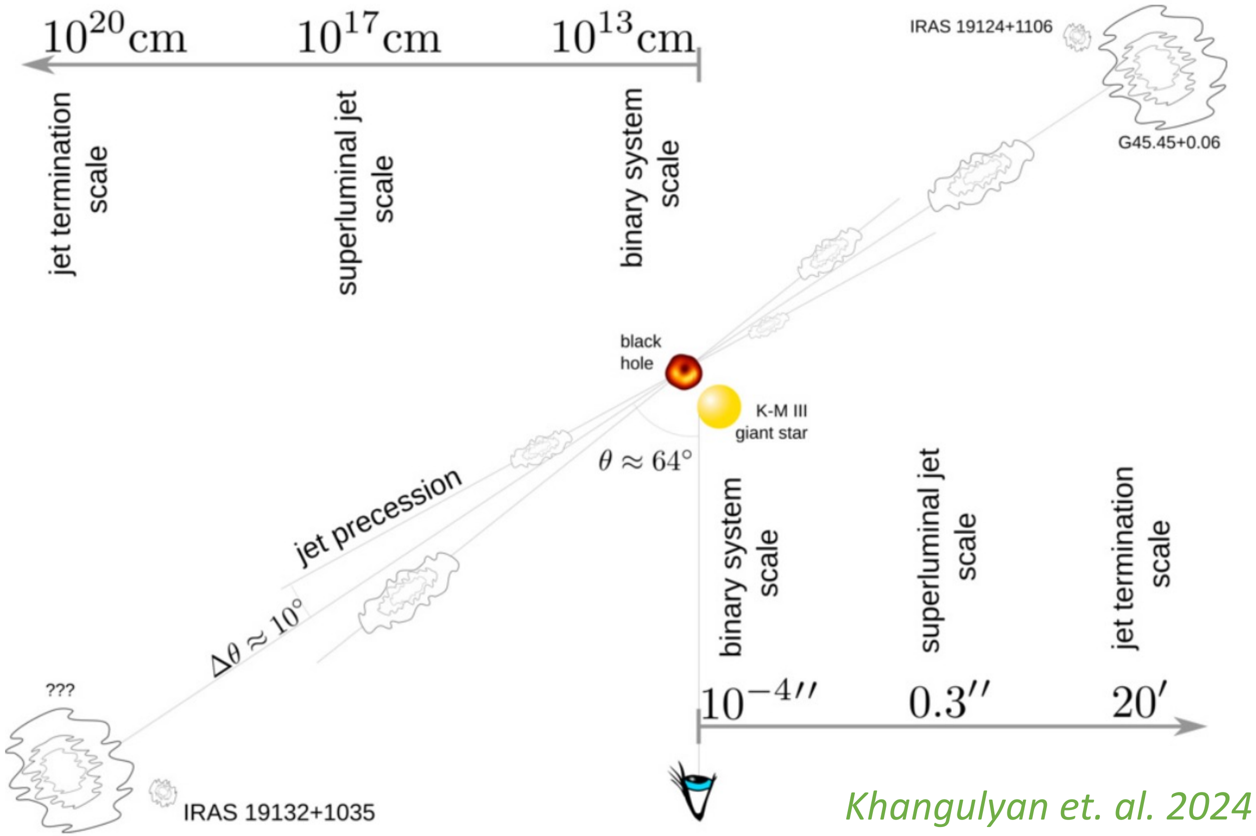

Khangulyan et. al. 2024

A candidate jet–ISM interaction spot with the counter-jet was identified to the north-west of GRS 1915+105 (IRAS 19124+1106)

- Not detect any radio lobe near IRAS 19124

GRS 1915+105

GRS 1915+105 is a wide binary system, with a longest period of P = 33.85 ± 0.16 days, formation of unusually large and luminous accretion disk

- The mass of the black hole is around 12 $M_\odot$
- The spectral type of the donor star was identified to be a K-type star mass of 0.5$M_\odot$, making GRS 1915+105 a low-mass X-ray binary (LMXB).
- The **position angle of the jets has rotated counterclockwise by 24°** between 1994 and 2023.

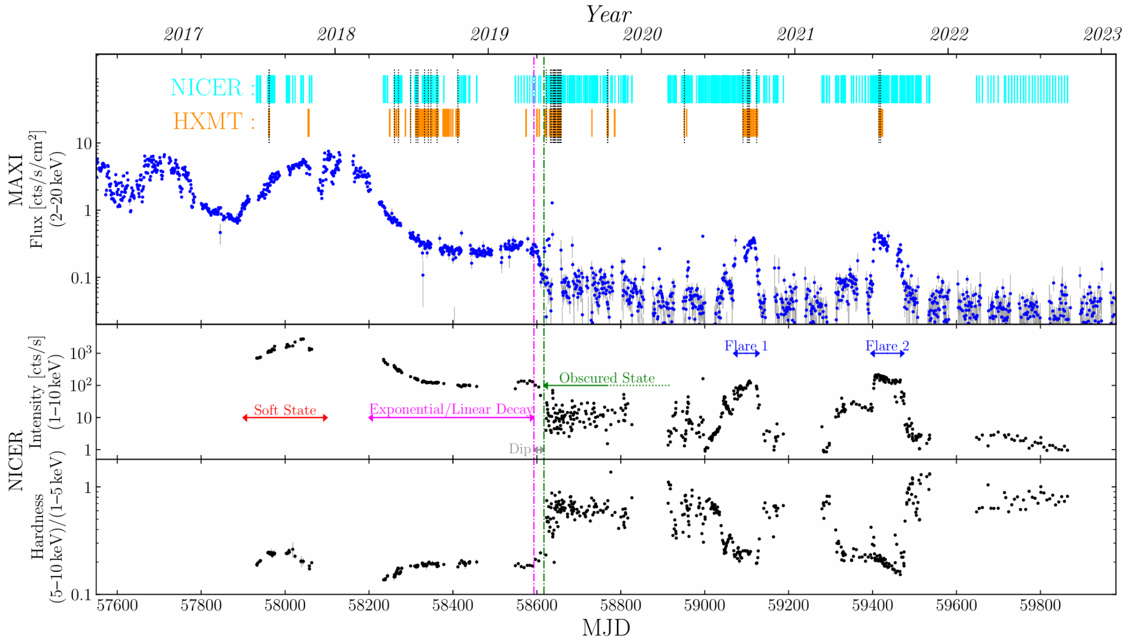

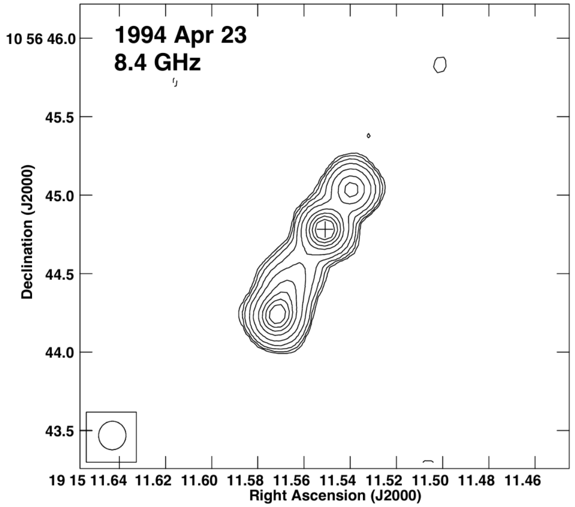

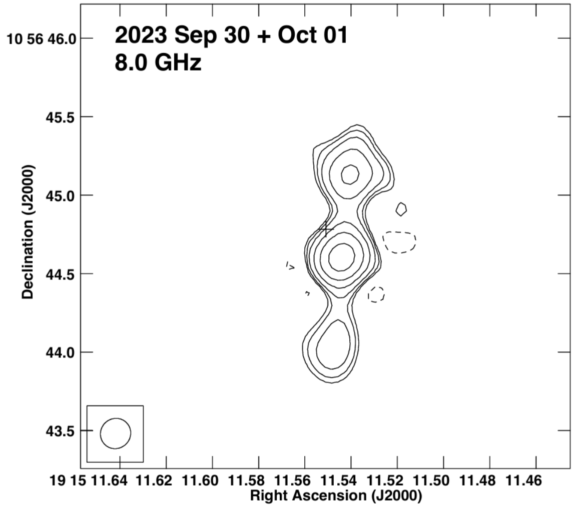

- Since its discovery in 1992, GRS 1915+105 remained one of the brightest black hole X-ray sources. It has remained in the outburst state since then. However, starting in 2018, its brightness started to decrease exponentially, then more gradually. By May 2019 (MJD 58617), it entered an obscured state, meaning its X-ray emissions became extremely faint.
- A Large Misalignment between Continuous Jet and Discrete Ejecta – *Jiang et al, 2026*

Progress on GRS1915+105 – LHAASO

- Detection at 1– 25 TeV band and increased sensitivity above 25 TeV

[LHAASO Colla, 2026, submitted]

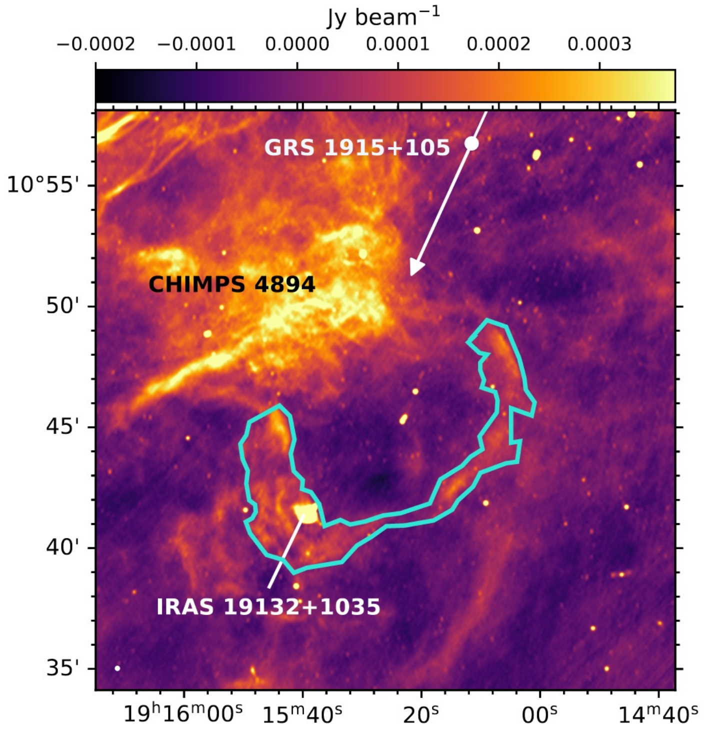

[Motta et. al. 2025]

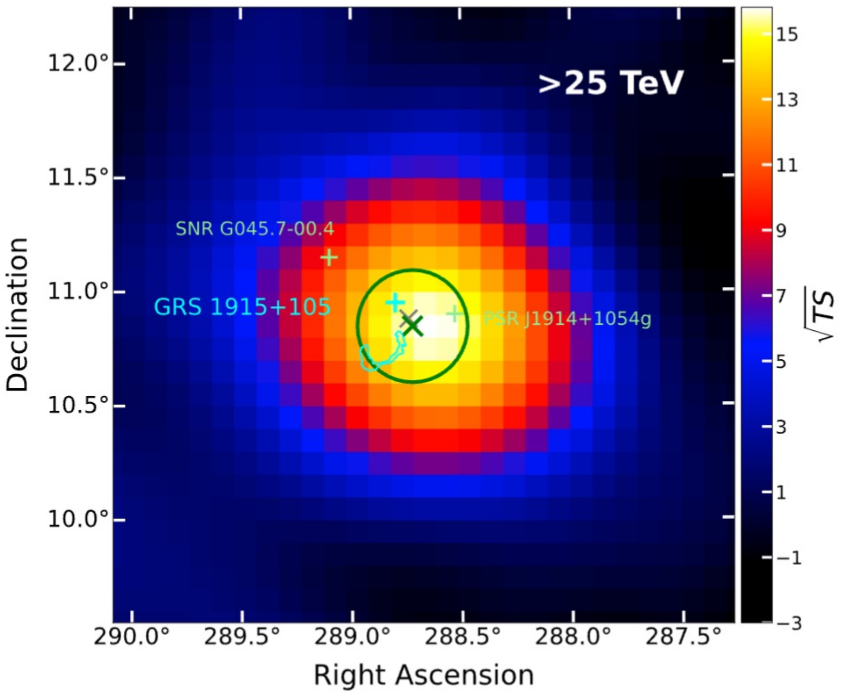

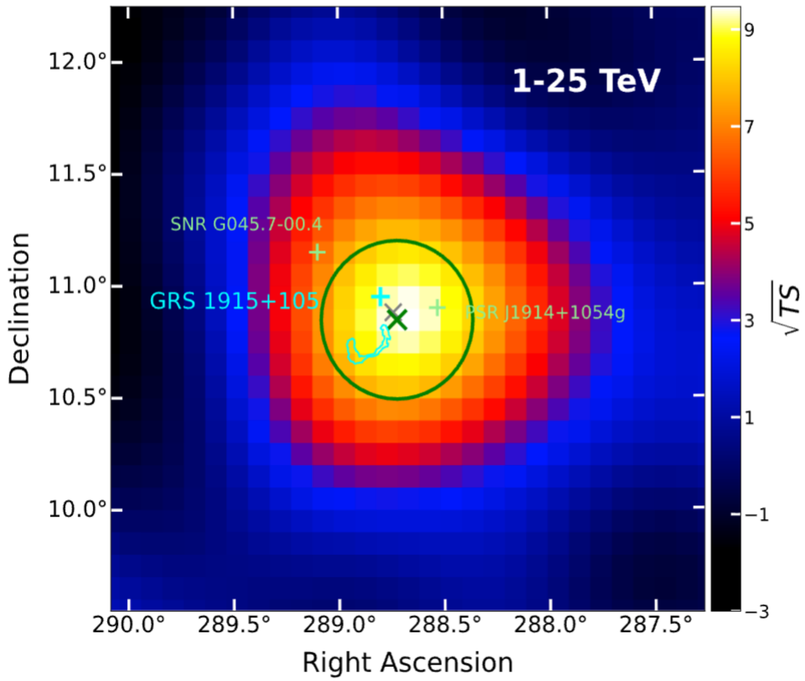

This work

Progress on GRS1915+105 – LHAASO + Fermi-LAT

[LHAASO Colla, 2026, submitted]

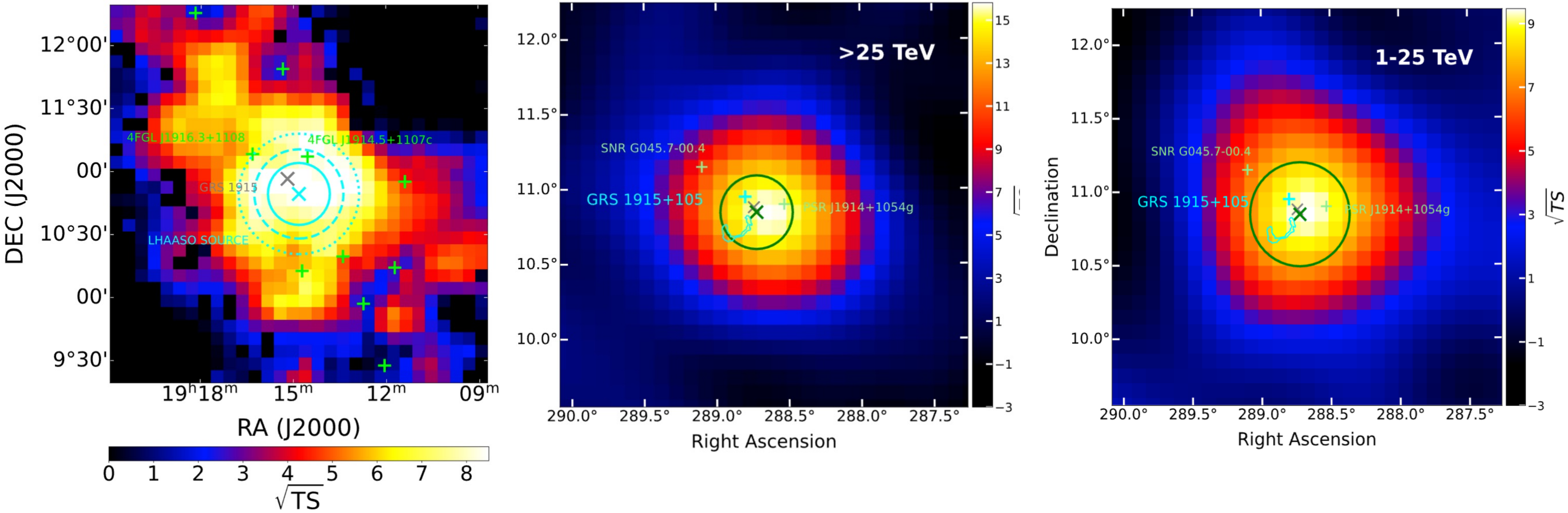

- The bow shock structure discovered by MeerKAT is well-aligned with LHAASO J1914+1050
- Analysis of Fermi-LAT data suggests a spatial extension that appears consistent with LHAASO measurements

UHE gamma rays from Microquasars

The origin of the non-thermal gamma rays in microquasars remains uncertain

- leptonic processes, including inverse Compton (IC) scattering from relativistic electrons (e.g., SS 433, V4641 Sgr) (Is hadronic model work?)

- Hadronic processes, involving proton synchrotron radiation, inelastic hadronuclear (pp) collisions, Bethe-Heitler (BH) pair production, and photomeson (pγ) interactions

(e.g., Cyg X-3 ! GRS 1915+105 !)

Inferred from the observation of by LHAASO:

- Microquasars are Galactic PeVatrons !!!

- Evidence of hadronic origin of UHE gamma-rays (Cyg X-3, GRS 1915+105)

But, CRs from microquasar could explain observed Galactic cosmic rays?

All-particle and helium spectrum

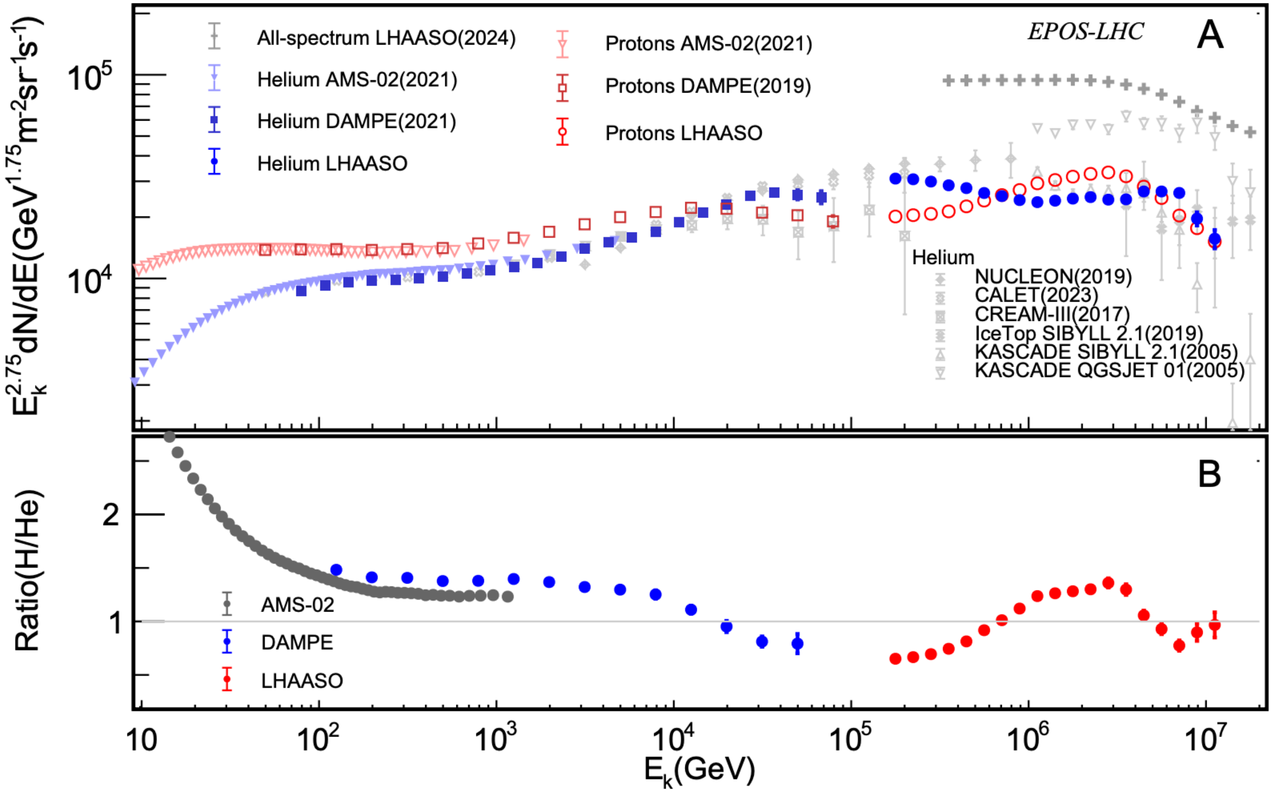

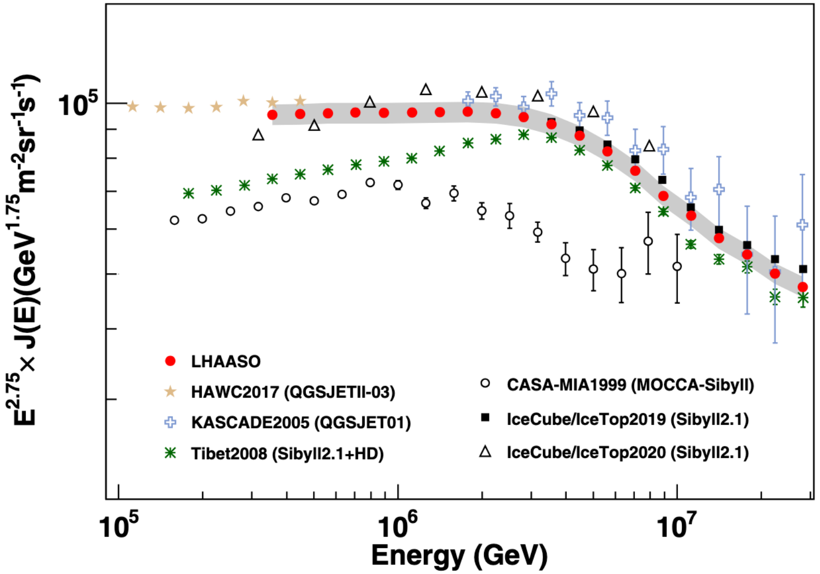

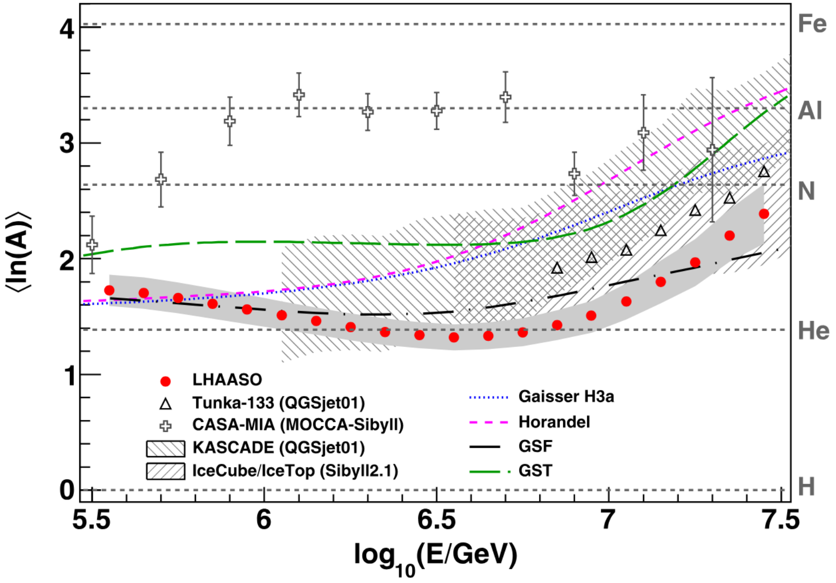

[LHAASO Collaboration, 2026, PRL, arXiv: 2511.05013]

[See also, LHAASO Collaboration, 2025, Sci. Bull. arXiv: 2505.14447]

But, CRs from microquasar could explain the observed all-particle cosmic ray spectrum and composition ?

Shear acceleration

Shear acceleration

- A class of the Fermi acceleration, has been suggested to be an efficient mechanism to accelerate CRs
- Charged particles gain energy inside an ordered shear velocity field

Ref. *Berezhko and G. F. Krymskii, 1981; Earl, J. R. Jokipii, ApJL, 1988; Ostrowski A&A, 1990; Webb ApJ, 1989; Rieger, Universe, 2019;*

Relativistic outflow speeds and sufficient energetic seed particle is needed to overcome adiabatic cooling

Extensive studies in radio galaxies

Application to mircoquasar system is possible

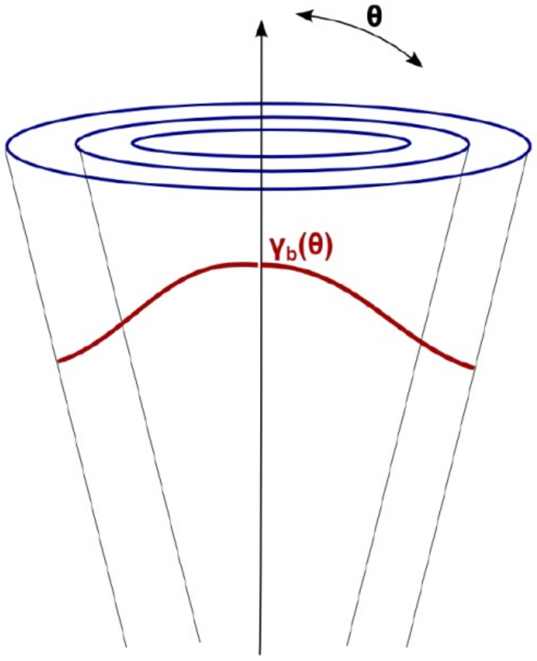

A simple conical flow whose radial outflow speeds varies with polar angle θ

Rieger, Universe, 2019

Discrete shear acceleration and CR injection

CRs will undergo a discrete shear acceleration, when the CR mean free path is longer than the width of the sheath layer: $\lambda \gtrsim r_{\rm sl}$

- The mean free path of CRs: $\lambda \sim l_{\rm coh}(E/E_{\rm coh})^{\delta}$
- For Kolmogorov turbulence: $\delta = 1/3$
- The coherence length inside the cocoon: $l_{\rm coh} \sim 0.03 r_{\rm coc} \sim 1.8$ pc
- The typical energy: $E_{\rm coh} = ZeB_{\rm coc}l_{\rm coh} \sim 17Z(B_{\rm coc}/10\ \mu{\rm G})(l_{\rm coh}/1.8\ {\rm pc})\ {\rm PeV}$
- The width of the sheath layer: $r_{\rm sl} \sim f_{\rm sl} r_{\rm jet} \sim 0.06(f_{\rm sl}/0.02)\ {\rm pc}$

The injection energy is given by $\lambda \sim r_{\rm sl}$

$$E_{\rm inj} \approx E_{\rm coh}\left(\frac{r_{\rm sl}}{l_{\rm coh}}\right)^3 \sim 0.6\left(\frac{B_{\rm coc}}{10\mu{\rm G}}\right)\left(\frac{r_{\rm sl}}{0.06\ {\rm pc}}\right)^3\left(\frac{l_{\rm coh}}{1.8{\rm pc}}\right)^{-2}\ {\rm TeV}$$

CRs with energies above several hundreds of GeV can undergo a discrete shear acceleration mechanism

Distances

TABLE S1. Galactic coordinates and distances for some microquasars, ordered by proximity to the Sun. The Galactic Center is provided for reference.

Source Name	l (°)	b (°)	d (kpc)
V616 Mon [26]	210.04	−6.54	1.06
XTE J1118+480 [27]	157.69	+62.31	1.72
Cygnus X-1 [28]	71.33	+3.07	2.22
V404 Cygni [29]	73.12	−2.07	2.39
GRO J0422+32 [45]	165.88	−11.91	2.49
GS 2000+251 [46]	63.37	−3.01	2.70
Scorpius X-1 [47]	359.09	+23.78	2.80
MAXI J1820+070 [48]	43.83	+5.29	2.96
GRO J1655−40 [49]	344.98	+2.46	3.20
4U 1755−33 [50]	357.22	−4.87	4.00
CI Cam [51]	148.47	+4.26	4.10
XTE J1550−564 [52]	325.88	−1.84	4.38
SS 433 [53]	39.70	−2.20	4.90
V4641 Sgr [54]	6.77	−4.79	6.20
XTE J1859+226 [55]	54.05	+8.61	8.00
GX 339−4 [56]	339.86	−4.32	8.40
Galactic Center	0.00	0.00	8.50
GRS 1915+105 [57, 58]	45.40	−0.20	9.40
Cygnus X-3 [59]	79.85	+0.68	9.40
Circinus X-1 [60]	322.12	−0.03	9.40
4U 1630−47 [61]	336.91	+0.25	11.50

X-ray binaries

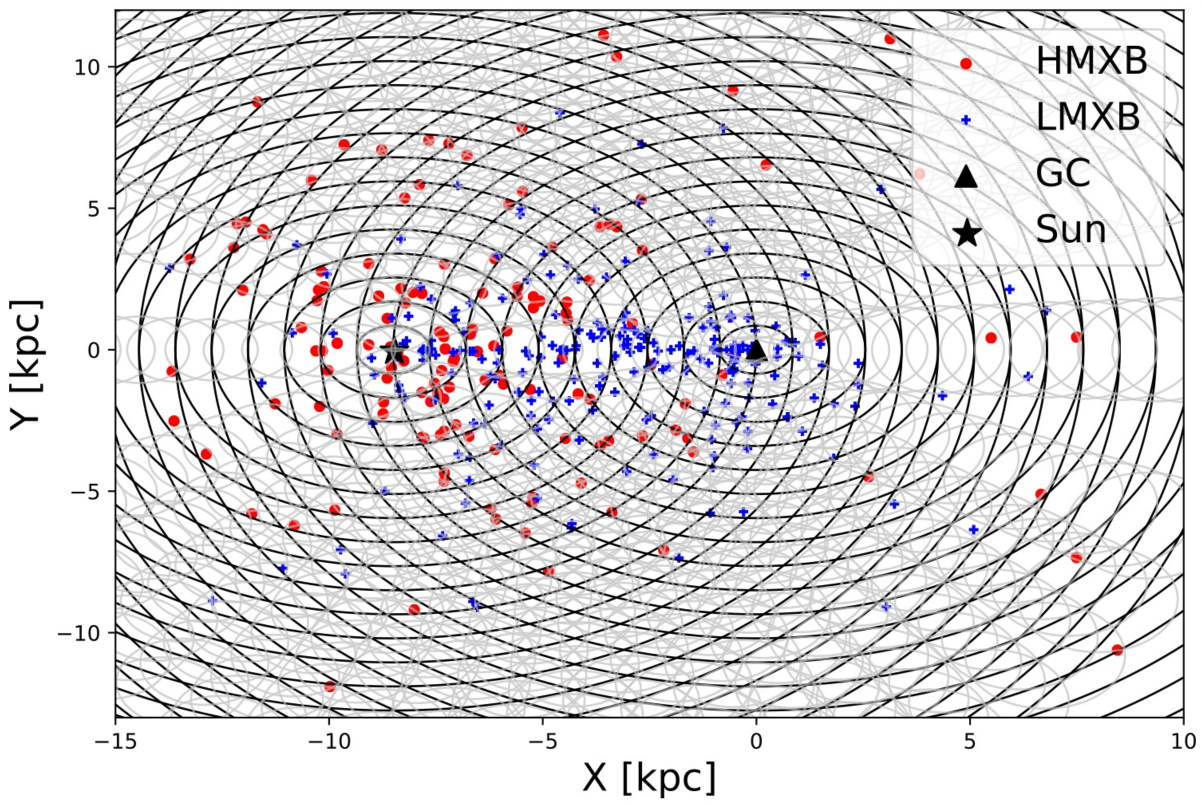

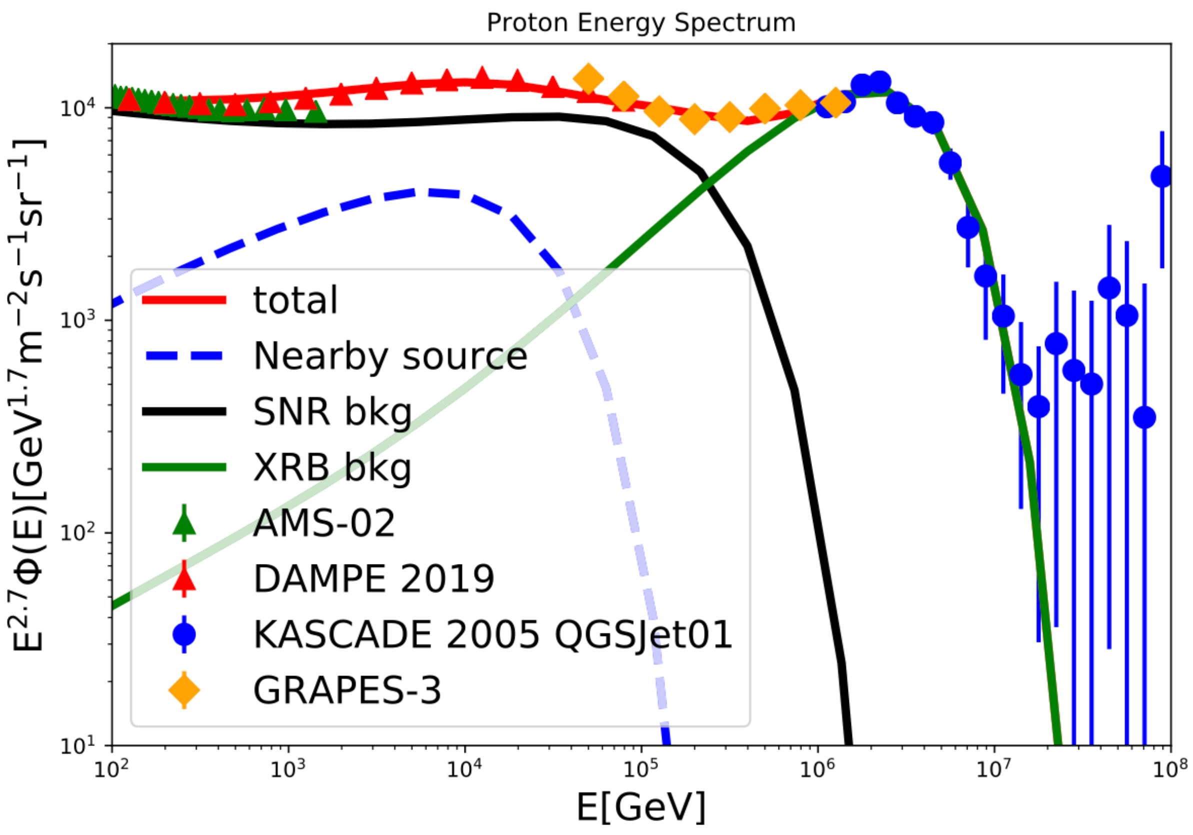

An overall picture of CRs from GeV to 100 EeV

Could we have an overall picture of CRs from GeV to 100 EeV?

A data-driven parameterization of cosmic-ray flux and mass composition: Global Spline Fit (GSF)

Fujisue, Dembinski, Engel, Fedynitch, UHECR, PoS, 2024